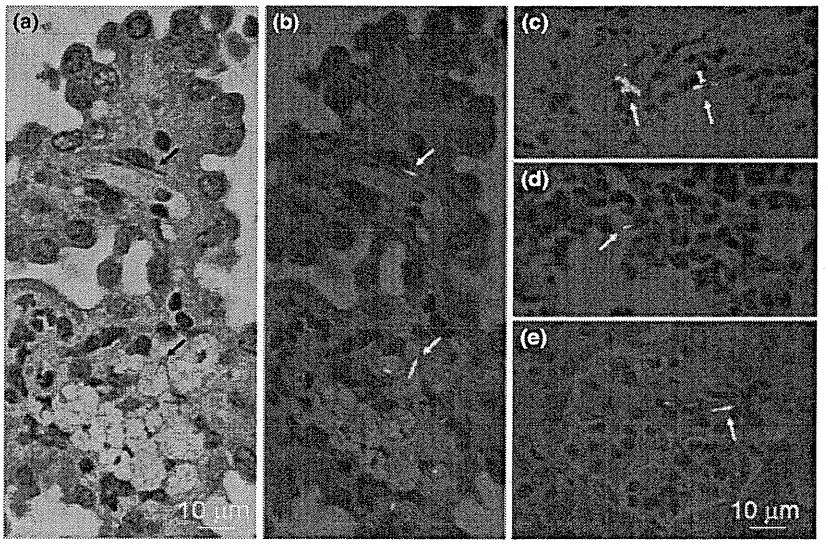

Fig. 5. Systemic distribution of singular fibers. Single micrometer-sized multi-wall carbon nanotube fibers are found in the choroid plexus in (a) normal lighting and (b) polarized light (in a mouse from the high-dose group sampled on day 168), (c) lung as an agglomerate within macrophages (polarized light) or (d) as singular fibers (polarized light) and (e) a renal glomerulus (polarized light) (in a mouse from the high-dose group sampled on day 197). Fibers were also found in hepatic sinusoids and mesenteric lymph nodes (not shown).

It is noted that the mesotheliomas of the low-dose group were not accompanied by foreign body granulomas or fibrous scars. The mesothelial atypical hyperplasia found 1 year after the i.p. injection in the low-dose group mice were also devoid of foreign body granulomas and fibrous scars. Instead, these lesions were backed up by an accumulation of mononuclear inflammatory cells. The macrophage-like cells in the accumulation, negative to weakly positive for F8/40, were often positive for singular MWCNT in their cytoplasm. As the mesothelial atypical hyperplasia is considered as precancerous lesions, the essential background of mesotheliomagenesis might be the inflammatory lesions without granulomas and fibrous scars formed against MWCNT agglomerates. The mesothelial atypical hyperplasia can be regarded as a lesion driven by the frustrated phagocytosis against MWCNT.

In general, carcinogenesis is considered a multistage process. In the case of chemical carcinogens with clear genotoxic properties, tumor onset occurs significantly earlier at higher doses.[19,20] Presumably, an increasing number of hits to a target cell leads to faster progression of the carcinogenic stages. Here, in contrast, the onset time of the mesotheliomas was apparently dose independent. Onset estimates calculated as x-intercepts of logarithmic approximation[21,22] were 126, 146, 148 and 138 days for the previous study data[2] and the three doses of the present study, respectively (Fig. S1). Mechanistically, a direct effect to a mesothelial cell, such as mutagenic or clastogenic effect, would favor a dose-dependent acceleration of the onset. If the granulomas are an important promoting factor of mesotheliomagenesis,[23] the highest dose group should have had the earliest onset because the granuloma formation can take place within 7 days subsequent to the i.p. injection.[24] In contrast, the humoral stimuli released from the nearby macrophages in the condition of frustrated phagocytosis[25] would match with this finding. As shown in Figures 3 and 4, the reactive mesothelial cells are accompanied by mononuclear inflammatory cells with MWCNT fibers, but not by epithelioid cell granulomas or fibrous scars. One could speculate that each loci of frustrated phagocytosis could continuously stimulate the nearby mesothelial cells, that is, first to induce reactive hyperplasia and then as the next step proceed towards mesothelioma. If the dose is the determinant of the number of such loci within a defined surface area of peritoneal mesothelial membrane, then it is natural to predict that the earliest day of tumor onset is dose independent, whereas the probability of tumor onset closer to the earliest day will increase in a dose-dependent manner.

An additional finding was the distribution of singular fibers to systemic organs such as the liver, mesenteric lymph nodes, pulmohilar lymph nodes, choroid plexus of the brain, glomeruli of the kidney and lung alveoli (Fig. 5). Because the brain, including the choroid plexus, lacks afferent lymphatics,[17,18] it is probable that the fibers were distributed systemically via the blood stream. Its importance to human health could be closely linked to the systemic distribution of asbestos reported in humans,[26,27] that is, a possibility of increasing systemic diseases such as cancer in various organs[28] and autoimmune diseases.[29] *In vivo* studies on the shorter fractions of MWCNT for its systemic toxicity would be essential.

It is likely that the peritoneal cavity served as a filter to segregate large agglomerates from the i.p. injected MWCNT suspension by the formation of foreign body granulomas and fibrous scars, leaving singular long MWCNT fibers for mesotheliomagenesis (frustrated phagocytosis) and short singular fibers for systemic distribution. The short fibers might have passed through the stomata (pores) of the mesothelium[23] or been transported by macrophages into lymphatics and to the vascular systems. As a whole, the i.p. injection model appears to be a robust system for the hazard identification of fiber carcinogenesis of asbestos-like fibrous particulate matter and of systemic toxicity of fibrous and non-fibrous particulate matter including nanoparticles that can enter the blood stream.

In conclusion, μm-MWCNT was mesotheliomagenic in the p53+/− mouse peritoneal cavity model in a dose-dependent manner from as low as 3 μg per mouse or approximately 10^6 fibers per mouse. Although the molecular mechanisms of fiber mesotheliomagenesis are unknown, the minute lesions seen in the lowest dose group and the dose-response characteristics might be consistent with the concept of frustrated phagocytosis and also with the observation in human asbestos epidemiology

that there would be no practical threshold for fiber mesotheliomagenesis.

Acknowledgments

The authors thank Mr Masaki Tsuji for technical support, and Dr Robert R. Maronpot and Dr Kai Savolainen for critical reading of the manuscript. The present study was supported by Health Sciences Research Grants H18-kagaku-ippan-007 and H21-kagaku-ippan-008 from the Ministry of Health, Labour and Welfare, Japan.

Disclosure Statement

The authors have no conflict of interest.

References

1 Service RF. CHEMISTRY: nanotubes: the next asbestos? *Science* 1998; **281**: 941.
2 Takagi A, Hirose A, Nishimura T *et al.* Induction of mesothelioma in p53+/− mouse by intraperitoneal application of multi-wall carbon nanotube. *J Toxicol Sci* 2008; **33**: 105–16.
3 Stanton MF, Layard M, Tegeris A *et al.* Relation of particle dimension to carcinogenicity in amphibole asbestoses and other fibrous minerals. *J Natl Cancer Inst* 1981; **67**: 965–75.
4 Pott F, Roller M, Kamino K, Bellmann B. Significance of durability of mineral fibers for their toxicity and carcinogenic potency in the abdominal cavity of rats in comparison with the low sensitivity of inhalation studies. *Environ Health Perspect* 1994; **102**(Suppl 5): 145–50.
5 Adachi S, Yoshida S, Kawamura K *et al.* Inductions of oxidative DNA damage and mesothelioma by crocidolite, with special reference to the presence of iron inside and outside of asbestos fiber. *Carcinogenesis* 1994; **15**: 753–8.
6 Roller M, Pott F, Kamino K, Althoff GH, Bellmann B. Dose-response relationship of fibrous dusts in intraperitoneal studies. *Environ Health Perspect* 1997; **105**(Suppl 5): 1253–6.
7 World Health Organization. *WHO Workshop on Mechanisms of Fibre Carcinogenesis and Assessment of Chrysotile Asbestos Substitutes*, 8–12 November 2005. Lyon, France: Summary Consensus Report World Health Organization, 2006.
8 European Chemicals Bureau. Carcinogenicity of synthetic mineral fibres after intraperitoneal injection in rats (ECB/TM/18(97) rev. 1). In: Bernstein DM, Riego Sintes JM, eds. *Methods for the Determination of the Hazardous Properties for Human Health of Man Made Mineral Fibres (MMMF) (EUR 18748 EN [1999])*. Ispra, Italy: Institute for Health and Consumer Protection, Unit: Toxicology and Chemical Substances, 1999; 41–52. [Cited 26 May 2012.] Available from URL: http://tsar.jrc.ec.europa.eu/documents/Testing-Methods/mmmfweb.pdf.
9 Marsella JM, Liu BL, Vaslet CA, Kane AB. Susceptibility of p53-deficient mice to induction of mesothelioma by crocidolite asbestos fibers. *Environ Health Perspect* 1997; **105**(Suppl 5): 1069–72.
10 Mahler JF, Flagler ND, Malarkey DE, Mann PC, Haseman JK, Eastin W. Spontaneous and chemically induced proliferative lesions in Tg.AC transgenic and p53-heterozygous mice. *Toxicol Pathol* 1998; **26**: 501–11.
11 Eastin WC, Haseman JK, Mahler JF, Bucher JR. The National Toxicology Program evaluation of genetically altered mice as predictive models for identifying carcinogens. *Toxicol Pathol* 1998; **26**: 461–73.
12 Tsukada T, Tomooka Y, Takai S *et al.* Enhanced proliferative potential in culture of cells from p53-deficient mice. *Oncogene* 1993; **8**: 3313–22.
13 Chung A, Cagle PT, Roggli VL, eds. *Tumors of the Serosal Membranes*. Washington, DC: American Registry of Pathology, 2006.
14 Chalabreysse L, Guillaud C, Tabib A, Loire R, Thivolet-Bejui F. Malignant mesothelioma with osteoblastic heterologous elements. *Ann Pathol* 2001; **21**: 428–30.
15 Matsukuma S, Aida S, Hata Y, Sugiura Y, Tamai S. Localized malignant peritoneal mesothelioma containing rhabdoid cells. *Pathol Int* 1996; **46**: 389–91.
16 Ordonez NG. Mesothelioma with rhabdoid features: an ultrastructural and immunohistochemical study of 10 cases. *Mod Pathol* 2006; **19**: 373–83.
17 Courtice FC, Simmonds WJ. The removal of protein from the subarachnoid space. *Aust J Exp Biol Med Sci* 1951; **29**: 255–63.
18 Weller RO, Djuanda E, Yow HY, Carare RO. Lymphatic drainage of the brain and the pathophysiology of neurological disease. *Acta Neuropathol* 2009; **117**: 1–14.
19 National Toxicology Program. NTP technical report on the toxicology and carcinogenesis studies of dimethyl vinyl chloride (L-chloro-2-methylpropene) (Cas No. 513-37-1) in F344/N rats and B6C3F1 mice (Gavage Studies) (NTP TR 316). National Toxicology Program, Research Triangle Park, North Carolina, 1986. [Cited 26 May 2012.] Available from URL: http://ntp.niehs.nih.gov/ntp/htdocs/lt_rpts/tr316.pdf.
20 National Toxicology Program. NTP technical report on the toxicology and carcinogenesis studies of glycidol (Cas No. 556-52-5) in F344/N rats and B6C3F1 mice (Gavage Studies) (NTP TR 374). National Toxicology Program, Research Triangle Park, North Carolina, 1990. [Cited 26 May 2012.] Available from URL: http://ntp.niehs.nih.gov/ntp/htdocs/LT_rpts/tr374.pdf.
21 Boffetta P, Burdorf A, Goldberg M, Merler E, Siemiatycki J. Towards the coordination of European research on the carcinogenic effects of asbestos. *Scand J Work Environ Health* 1998; **24**: 312–7.
22 Yano E, Wang ZM, Wang XR, Wang MZ, Lan YJ. Cancer mortality among workers exposed to amphibole-free chrysotile asbestos. *Am J Epidemiol* 2001; **154**: 538–43.
23 Donaldson K, Murphy FA, Duffin R, Poland CA. Asbestos, carbon nanotubes and the pleural mesothelium: a review of the hypothesis regarding the role of long fibre retention in the parietal pleura, inflammation and mesothelioma. *Part Fibre Toxicol* 2010; **7**: 5.
24 Poland CA, Duffin R, Kinloch I *et al.* Carbon nanotubes introduced into the abdominal cavity of mice show asbestos-like pathogenicity in a pilot study. *Nat Nanotechnol* 2008; **3**: 423–8.
25 Nagai H, Toyokuni S. Biopersistent fiber-induced inflammation and carcinogenesis: lessons learned from asbestos toward safety of fibrous nanomaterials. *Arch Biochem Biophys* 2010; **502**: 1–7.
26 Tossavainen A, Karjalainen A, Karhunen PJ. Retention of asbestos fibers in the human body. *Environ Health Perspect* 1994; **102**(Suppl 5): 253–5.
27 Miserocchi G, Sancini G, Mantegazza F, Chiappino G. Translocation pathways for inhaled asbestos fibers. *Environ Health* 2008; **7**: 4.
28 Goldsmith JR. Asbestos as a systemic carcinogen: the evidence from eleven cohorts. *Am J Ind Med* 1982; **3**: 341–8.
29 Noonan CW, Pfau JC, Larson TC, Spence MR. Nested case-control study of autoimmune disease in an asbestos-exposed population. *Environ Health Perspect* 2006; **114**: 1243–7.

Supporting Information

Additional Supporting Information may be found in the online version of this article:

Fig. S1. Estimation of the time of tumor onset.

Please note: Wiley-Blackwell are not responsible for the content or functionality of any supporting materials supplied by the authors. Any queries (other than missing material) should be directed to the corresponding author for the article.

doi: 10.1111/j.1349-7006.2012.02318.x

Cancer Science
The official journal of the Japanese Cancer Association

Multi-walled carbon nanotubes translocate into the pleural cavity and induce visceral mesothelial proliferation in rats

Jiegou Xu,[1,2] Mitsuru Futakuchi,[2] Hideo Shimizu,[3] David B. Alexander,[1] Kazuyoshi Yanagihara,[4] Katsumi Fukamachi,[2] Masumi Suzui,[2] Jun Kanno,[5] Akihiko Hirose,[6] Akio Ogata,[7] Yoshimitsu Sakamoto,[7] Dai Nakae,[7] Toyonori Omori[8] and Hiroyuki Tsuda[1,9]

[1]Laboratory of Nanotoxicology Project, Nagoya City University, Nagoya; [2]Department of Molecular Toxicology; [3]Core Laboratory, Nagoya City University Graduate School of Medical Sciences, Nagoya; [4]Department of Life Sciences, Yasuda Women's University Faculty of Pharmacy, Hiroshima; [5]Division of Cellular and Molecular Toxicology; [6]Division of Risk Assessment, National Institute of Health Sciences, Tokyo; [7]Department of Pharmaceutical and Environmental Sciences, Tokyo Metropolitan Institute of Public Health, Tokyo; [8]Department of Health Care Policy and Management, Nagoya City University Graduate School of Medical Sciences, Nagoya, Japan

(Received July 17, 2012/Revised August 20, 2012/Accepted August 22, 2012/Accepted manuscript online August 31, 2012/Article first published online October 10, 2012)

Multi-walled carbon nanotubes have a fibrous structure similar to asbestos and induce mesothelioma when injected into the peritoneal cavity. In the present study, we investigated whether carbon nanotubes administered into the lung through the trachea induce mesothelial lesions. Male F344 rats were treated with 0.5 mL of 500 μg/mL suspensions of multi-walled carbon nanotubes or crocidolite five times over a 9-day period by intrapulmonary spraying. Pleural cavity lavage fluid, lung and chest wall were then collected. Multi-walled carbon nanotubes and crocidolite were found mainly in alveolar macrophages and mediastinal lymph nodes. Importantly, the fibers were also found in the cell pellets of the pleural cavity lavage, mostly in macrophages. Both multi-walled carbon nanotube and crocidolite treatment induced hyperplastic proliferative lesions of the visceral mesothelium, with their proliferating cell nuclear antigen indices approximately 10-fold that of the vehicle control. The hyperplastic lesions were associated with inflammatory cell infiltration and inflammation-induced fibrotic lesions of the pleural tissues. The fibers were not found in the mesothelial proliferative lesions themselves. In the pleural cavity, abundant inflammatory cell infiltration, mainly composed of macrophages, was observed. Conditioned cell culture media of macrophages treated with multi-walled carbon nanotubes and crocidolite and the supernatants of pleural cavity lavage fluid from the dosed rats increased mesothelial cell proliferation *in vitro*, suggesting that mesothelial proliferative lesions were induced by inflammatory events in the lung and pleural cavity and likely mediated by macrophages. In conclusion, intrapulmonary administration of multi-walled carbon nanotubes, like asbestos, induced mesothelial proliferation potentially associated with mesothelioma development. (*Cancer Sci* 2012; 103: 2045–2050)

Multi-walled carbon nanotubes (MWCNT) are structurally composed of cylinders rolled up from several layers of graphite sheets. They are several to tens of nanometers in diameter and several to tens of micrometers in length. This high length to diameter aspect ratio, a characteristic shared with asbestos fibers, has led to concern that exposure to MWCNT might cause asbestos-like lung diseases, such as lung fibrosis, lung cancer, pleural plaque and malignant mesothelioma.[1–6]

Pleural plaque and malignant mesothelioma are characteristic lesions in asbestos-exposed humans. Although fiber dimensions, biopersistence, oxidative stress and inflammation have all been implicated,[7–12] the exact mechanisms of pleural pathogenesis are unclear. According to a pathogenesis paradigm suggested by Donaldson *et al.*,[2] asbestos fibers penetrate into the pleural cavity from the alveoli and deposit in the pleural tissue. Unlike spherical particles, fibrous materials such as asbestos are not cleared effectively from the pleural cavity, resulting in deposition of the fibers in the parietal pleura. This deposition, in turn, causes frustrated phagocytosis-induced pro-inflammatory, genotoxic and mitogenic responses in the deposition sites.[2]

Administration of MWCNT into the peritoneal cavity or scrotum in animals has been reported to induce mesothelial lesions, similar to those observed in asbestos cases.[13–15] The induction of mesothelioma in the peritonum is dose dependent, and is observed with as low as 3 μg/mouse in p53 heterozygous mice.[16] These studies suggest a potential risk that inhaled MWCNT might lead to pleural mesothelioma. However, actual experimental evidence demonstrating induction of pleural mesothelioma by inhaled MWCNT fibers has not yet been shown. It has been shown that inhaled MWCNT induced subpleural fibrosis with macrophage aggregates on the surface of the visceral pleura.[17] Notably, some of these macrophages contained MWCNT fibers. In addition, penetration of MWCNT administrated by pharyngeal aspiration into the pleural cavity was observed,[18] and intrapleural injection of 5 μg/mouse of MWCNT has been shown to lead to sustained inflammation and length-dependent retention of MWCNT in the pleural cavity.[19] Accordingly, direct interaction of MWCNT with the mesothelial tissue is postulated as an early pathogenic event.

In the present study, to examine whether MWCNT translocate into the pleural cavity and cause inflammation leading to proliferative change of the mesothelial tissue, we administered relatively high doses (five doses at 250 μg/rat) of two MWCNT samples (MWCNT-N and MWCNT-M) to the rat lung by intrapulmonary spraying (IPS)/intratracheal instillation; crocidolite (CRO; one kind of asbestos fiber) was used as a positive control. Intrapulmonary spraying has been shown to be an efficient method to deliver particle materials deep into the lung.[20–24] Our results demonstrated that MWCNT, like asbestos, translocated from the lung into the pleural cavity and induced inflammatory responses in the pleural cavity and, importantly, hyperplastic visceral mesothelial proliferation. These findings are important in understanding whether MWCNT have the potential to cause asbestos-like pleural lesions.

[9]To whom correspondence should be addressed.
E-mail: htsuda@phar.nagoya-cu.ac.jp

doi: 10.1111/cas.12005

Materials and Methods

Animals. Eight-week-old male F344 rats were purchased from Charles River Japan Inc. (Kanagawa, Japan). The animals were housed in the Animal Center of Nagoya City University Medical School and maintained on a 12 h light/12 h dark cycle, and received Oriental MF basal diet (Oriental Yeast Co. Ltd, Tokyo, Japan) and water *ad libitum*. The study was conducted according to the Guidelines for the Care and Use of Laboratory Animals of Nagoya City University Medical School and the experimental protocol was approved by the Institutional Animal Care and Use Committee (H22M-19).

Preparation of MWCNT and CRO suspensions. The MWCNT investigated were MWCNT-N (Nikkiso Co., Ltd, Tokyo, Japan) and MWCNT-7 (Mitsui Chemicals Inc., Tokyo, Japan; designated as MWCNT-M). Crocidolite (Union for International Cancer Control grade) was from the National Institute of Health Sciences of Japan stocks. Ten milligrams of MWCNT-N or MWCNT-M were suspended in 20 mL of saline containing 0.1% Tween 20 and homogenized for 1 min four times at 3000 r.p.m. in a Polytron PT1600E benchtop homogenizer (Kinematika AG, Littau, Switzerland). The suspensions were sonicated for 30 min shortly before use to minimize aggregation. The CRO suspension was prepared similarly, but without homogenization. The concentration of the MWCNT and CRO suspensions was 500 μg/mL. The lengths of MWCNT and CRO in the suspensions were determined using a digital map meter (Comcureve-9 Junior; Koizumi Sokki MFG. Co., Ltd, Nigata, Japan) on scanning electron microscope (SEM) photos. The SEM observation and length distributions of MWCNT and CRO are shown in Fig. S1A,B. To count the fiber number, 500 μg/mL suspensions of MWCNT-N, MWCNT-M and CRO were diluted 1:1000 with deionized water and 0.5 μL of the diluted suspensions was loaded onto clean glass slides and dried in a micro oven at 480°C for 1 min. The fiber number on the slides was counted under a polarized light microscope (PLM) (Olympus BX51N-31P-O PLM, Tokyo, Japan) (PLM detects all fibers longer than 200 nm). The results are shown in Fig. S1C.

Intrapulmonary spraying of MWCNT and CRO into the lung and pleural cavity lavage (PCL). We used the intrapulmonary spraying technique that was developed in our laboratory.[24] Briefly, rats were anaesthetized using isoflurane; the mouth was fully opened with the tongue gently held and the nozzle of a microsprayer (series IA-1B Intratracheal Aerosolizer; Penn-century, Philadelphia, PA, USA) was inserted into the trachea through the larynx and 0.5 mL suspension was sprayed into the lungs synchronizing with spontaneous respiratory inhalation. We confirmed that the dosed materials were distributed deep into the lung tissue and reached most of the terminal alveoli without causing obvious respiratory distress.

Ten-week-old male Fisher 344 rats were divided into four groups of six animals each and given 0.5 mL of saline containing 0.1% Tween 20 or 500 μg/mL MWCNT-N, MWCNT-M or CRO suspension by IPS once every other day five times over a 9-day period. The total amount of fibers administered was 1.25 mg/rat. Six hours after the last IPS, the rats were placed under deep isoflurane anesthesia; a small incision was made in the abdominal wall, the pleural cavity was injected with 10 mL of ice cold RPMI 1640 through the diaphragm, and the lavage fluid was collected by syringe. The rats were then killed by exsanguination from the inferior vena cava and the major organs, including the lung, chest wall, brain, liver, kidney, spleen and mediastinal lymph nodes, were fixed in 4% paraformaldehyde and processed for histological examination.

Analysis of inflammatory reaction in the pleural cavity. Cells in the lavage fluid were counted using a hemocytometer (Erma Co., Ltd, Tokyo, Japan), and the cellular fraction was then isolated by centrifugation at 200*g* for 5 min at 4°C. Cell pellets collected from three rats were combined (generating a total of two cell pellets per group), fixed in 4% paraformaldehyde and processed for histological examination. Total protein in the supernatants of each of the lavage fluids was determined using the Pierce BCA Protein Assay Kit (Thermo Scientific, Rockford, IL, USA) and the supernatants were then concentrated by centrifugation in Vivaspin 15 concentrators (Sartorius Stedium Biotech, Goettingen, Germany) at 1500*g* for 30 min at 4°C and used for *in vitro* cell proliferation assays.

Light microscopy and PLM. Haematoxylin–eosin (H&E)-stained slides of the lung tissues and cellular pellets of the PCL were used to observe MWCNT-N, MWCNT-M and CRO fibers with PLM at ×1000 magnification. The exact localization of the illuminated fibers was confirmed in the same H&E-stained sections after removing the polarizing filter.

Scanning electron microscopy. The H&E-stained slides of the lung tissue and PCL pellets were immersed in xylene for 3 days to remove the cover glass, then immersed in 100% ethanol for 10 min to remove the xylene and air-dried for 2 h at room temperature. The slides were then coated with platinum for viewing using a scanning electronic microscope (SEM) (Model S-4700 Field Emission SEM; Hitachi High Technologies Corporation, Tokyo, Japan) at 5–10 kV.

Immunohistochemistry and Azan–Mallory staining. CD68, proliferating cell nuclear antigen (PCNA) and mesothelin/Erc were detected using antirat CD68 antibodies (BMA Biomedicals, Augst, Switzerland), anti-PCNA monoclonal antibodies (Clone PC10; Dako Japan Inc., Tokyo, Japan) and antirat C-ERC/mesothelin polyclonal antibodies (Immuno-Biological Laboratories Co., Ltd, Gunma, Japan). The CD68, PCNA and C-ERC/mesothelin antibodies were diluted 1:100, 1:200 and 1:1000, respectively, in blocking solution and applied to deparaffinized slides. The slides were incubated at 4°C overnight and then incubated for 1 h with biotinylated species-specific secondary antibodies diluted 1:500 (Vector Laboratories, Burlingame, CA, USA) and visualized using avidin-conjugated horseradish peroxidase complex (ABC kit; Vector Laboratories). Azan–Mallory staining was used to visualize collagen fibers.

***In vitro* exposure and preparation of conditioned macrophage culture media.** The induction and preparation of primary alveolar macrophages (PAM) has been described previously.[24] PAM were seeded into 6 cm culture dishes at 2×10^6 cells per well in 10% FBS RPMI 1640. After overnight incubation, the culture media was refreshed and MWCNT-N, MWCNT-M or CRO suspensions were added to the cells to a final concentration of 10 μg/mL. The cells were then incubated for another 24 h. The conditioned macrophage culture media was then collected for *in vitro* cell proliferation assays.

***In vitro* cell proliferation assay.** Human mesothelioma cells, TCC-MESO1, derived from a patient in the Tochigi Cancer Center,[25] were seeded into 96-well culture plates at 2×10^3 cells per well in 10% FBS RPMI 1640. After overnight incubation, the cells were serum-starved for 24 h. The media was changed to 100 μL of the concentrated supernatants of the PCL or conditioned macrophage culture media and incubated for 72 h. The relative cell number was then determined using the Cell Counting Kit-8 (Dojindo Molecular Technologies, Rockville, MD, USA) according to the manufacturer's instruction.

Statistical analysis. Statistical analysis was performed using ANOVA. The statistical significance was analyzed using a two-tailed Student's *t*-test. A *P*-value of <0.05 was considered to be significant.

Results

Translocation of MWCNT and CRO fibers into the pleural cavity. The cell pellets of the PCL were used to examine whether

doi: 10.1111/cas.12005

the MWCNT or CRO fibers were present in the pleural cavity. We first screened the H&E-stained PCL cell pellet slides using PLM. The exact localization of the fibers was confirmed using SEM of the same slide sections. MWCNT-N, MWCNT-M and CRO fibers were present in PCL cell pellets, with most of the fibers in macrophage-like cells (Fig. 1a–c) with very few fibers located in the intercellular space or on cell surfaces (data not shown). Immunohistochemistry with CD68, a macrophage marker, showed that MWCNT and CRO fibers were mainly found in macrophages (Fig. 1d,e).

In tissue sections, MWCNT and CRO fibers were mainly detected in focal granulomatous lesions in the alveoli and in alveolar macrophages. Fibers were also found in the mediastinal lymph nodes, and a few fibers were detected in liver sinusoid cells, blood vessel wall cells in the brain, renal tubular cells and spleen sinus and macrophages (data not shown). We detected only a few fibers penetrating directly from the lung to the pleural cavity through the visceral pleura (Fig. S2) and did not find any fibers in the parietal pleura.

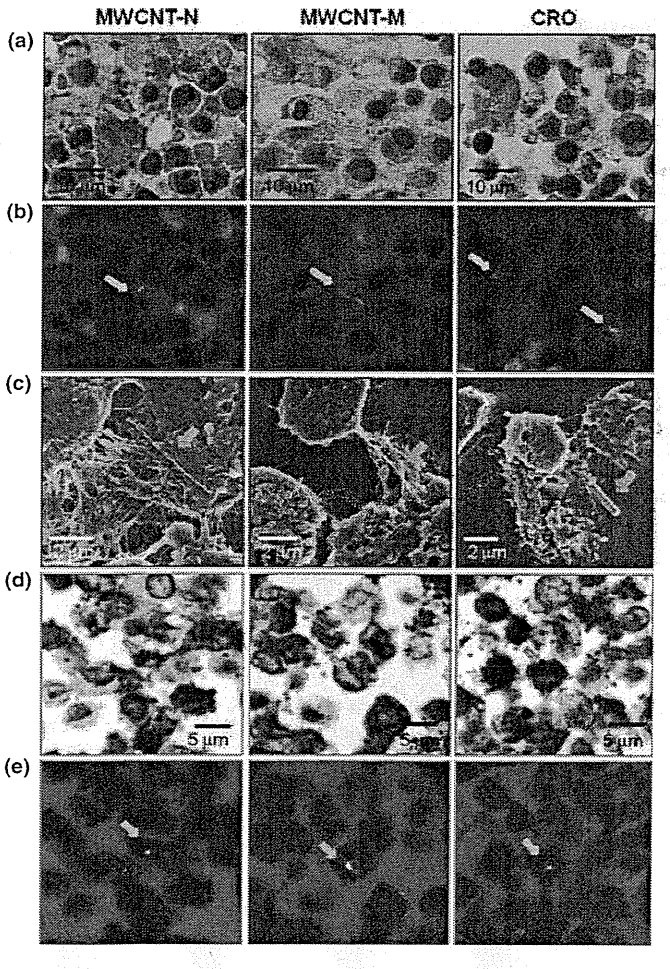

Fig. 1. Existence of multi-walled carbon nanotubes (MWCNT)-N, MWCNT-M and crocidolite (CRO) fibers in the cell pellets of the pleural cavity lavage (PCL). (a) Images of H&E-stained slides of the cell pellets of the PCL treated with MWCNT-N, MWCNT-M and CRO fibers. (b) Polarized light microscope (PLM) images of the same view areas shown in (a). (c) Scanning electron microscope observation showed the existence of the MWCNT and CRO fibers in the cell pellets of the PCL. (d) CD68 immunostaining of the PCL cell pellet slides. (e) PLM observation of the same view areas shown in (d) indicate that MWCNT and CRO fibers were present in the CD68-positive macrophages. Arrows indicate MWCNT-N, MWCNT-M and CRO fibers.

Induction of visceral mesothelial proliferation. Hyperplastic visceral mesothelial proliferation (HVMP) was clearly observed in all of the MWCNT and CRO treated groups. The HVMP lesions were composed of mesothelial cells with cuboidal appearance and increased size and density lining the visceral pleural tissue. Various degrees of lung inflammation and fibrous thickening were observed underneath the HVMP lesions (Fig. 2a, panel A). The PCNA immunostaining showed proliferating mesothelial cells within the HVMP lesions (Fig. 2a, panel B). The PCNA indices of the visceral mesothelium were increased approximately 10-fold in all the MWCNT and CRO treated groups compared with the control group

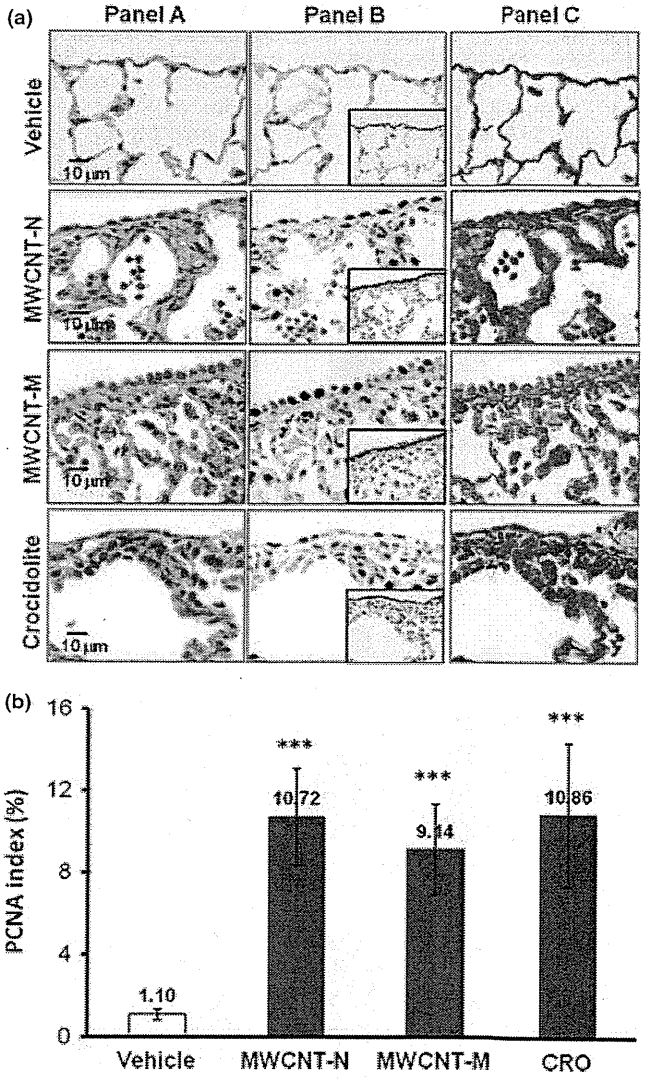

Fig. 2. Induction of visceral mesothelial cell proliferation lesions by treatment with multi-walled carbon nanotubes (MWCNT)-N, MWCNT-M or crocidolite (CRO). (a) Serial sections were prepared and stained with H&E, proliferating cell nuclear antigen (PCNA), Erc/mesothelin and Azan–Mallory's collagen staining. Panel A: increase in enlarged visceral mesothelial cells with cuboidal shapes in the MWCNT-N, MWCNT-M and CRO treated groups. Panel B: PCNA-positive cells are clearly increased in the dosed groups. The inserts are immunostained with Erc/mesothelin and show the lining of the mesothelium. Panel C: Azan–Mallory's staining; sub-pleural collagenous fibrosis is present under the mesothelial cell proliferation lesions. (b) PCNA index, expressed as the percentage of PCNA-positive cells of the total number of visceral mesothelial cells per slide. ***$P < 0.001$.

(Fig. 2b). Azan–Mallory staining showed increases in collagen fibers underneath the HVMP lesions (Fig. 2a, panel C). Fibers were not found within the HVMP lesions themselves. Alveolar macrophages with phagocytosed MWCNT or CRO fibers were frequently observed near the HVMP lesions (Fig. S3). Proliferation and other lesions of the parietal mesothelium were not observed.

Inflammatory cell infiltration in the pleural cavity. Both MWCNT and CRO treatment resulted in inflammatory reactions in the pleural cavity. The total number of cells, composed mostly of macrophages, neutrophils and lymphocytes, in the PCL in the MWCNT and CRO treated groups was significantly increased compared with the control group (Fig. 3a). As can be calculated from Fig. 3(a,b), macrophages accounted for a large part of the increase of the total cell number in the PCL, although the number of neutrophils and lymphocytes also increased. Overall, the proportion of macrophages in the cell pellets of the PCL was increased, while those of neutrophils and lymphocytes were decreased (Fig. 3b). MWCNT or CRO treatment also significantly increased the total protein level in the PLC (Fig. 3c). The proportion of cells in the PCL pellets positive for Mesothelin/Erc, a mesothelial cell marker, was 0.53–1.02%, and no intergroup difference was observed (data not shown). These data indicate that the increased cell number in the pleural cavity of the rats treated with MWCNT or CRO resulted from inflammatory cell effusion, not from mesothelial cell shedding of the pleural tissue. Many macrophages in the PCL contained MWCNT or CRO fibers.

Mesothelial cell proliferation assay *in vitro*. To examine whether inflammatory reactions, especially those mediated by macrophages, exert proliferative effects on mesothelial cells, we examined the effects of conditioned macrophage culture medium on mesothelial cell proliferation *in vitro*. The conditioned culture media of macrophages exposed to MWCNT-N, MWCNT-M or CRO significantly increased the proliferation of the human mesothelioma cell line TCC-MESO1. The concentrated supernatants of the PCL taken from the rats treated with MWCNT-N, MWCNT-M or CRO exhibited similar effects (Fig. 4). These results indicate that factors in the PCL, possibly secreted by alveolar and pleural macrophages, are able to cause mesothelial cell proliferation.

Discussion

In the present study, we compared the pleural translocation of MWCNT and CRO and examined the mesothelial lesions they induced. Our data demonstrate that after deposition in the lung, MWCNT, like CRO, translocated into the pleural cavity, mainly in pleural macrophages. Both MWCNT and CRO treatment also caused hyperplastic visceral mesothelial proliferation and marked pleural inflammation.

This is the first report to show that MWCNT administered into the rat lung causes mesothelial proliferative lesions. Adamson *et al.*[26] reported that intratracheal instillation of asbestos in mice induced pleural mesothelial cell proliferation within several days; the degree of pleural mesothelial cell proliferation did not appear to correlate with the localization of asbestos fibers in the pleura.[27] Similarly, we did not find fibers within the HVMP lesions. Thus, our findings suggest that HVMP lesions do not appear to be directly induced by the deposited MWCNT or CRO fibers. Also, *in vitro* exposure to MWCNT and CRO fibers did not lead to proliferation of TCC-MESO1 cells, but rather to cell death (Fig. S4). It has been reported that macrophages play a significant role in mesothelial cell proliferation caused by asbestos exposure and surgical injury,[28–31] and that the conditioned medium of macrophages

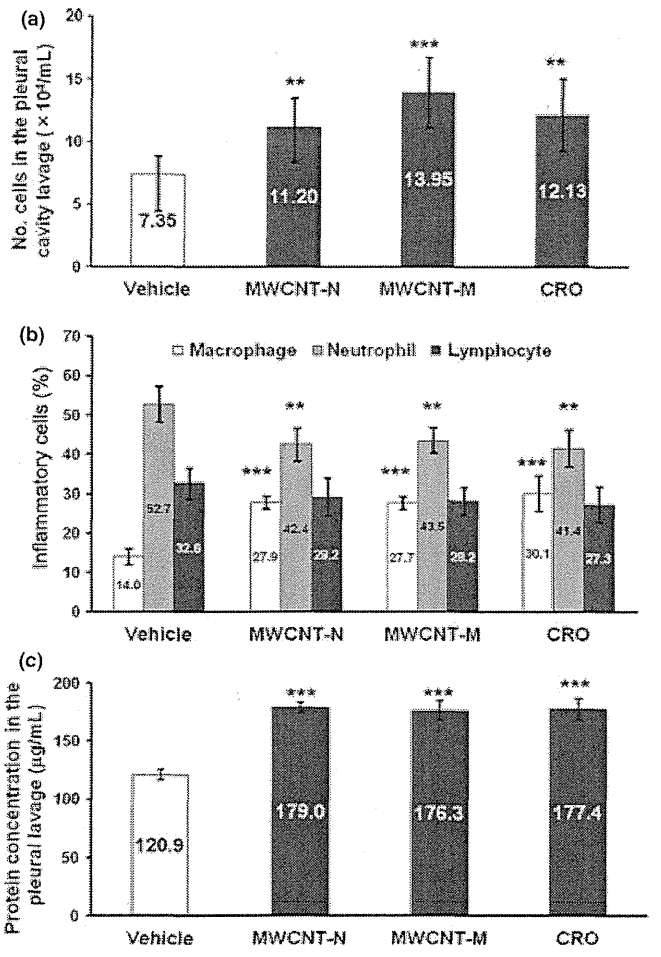

Fig. 3. Inflammatory reaction in the pleural cavity. (a) The number of leukocytes in the pleural cavity lavage (PCL) of rats treated with multi-walled carbon nanotubes (MWCNT) and crocidolite (CRO). (b) The proportion of macrophages, neutrophils and lymphocytes in the cell pellets of the PCL. Total cell number and cell numbers of macrophages, neutrophils and lymphocytes in 10 randomly chosen fields (×400) were counted. (c) Protein concentration in the supernatants of the PCL. $^{**}P < 0.01$; $^{***}P < 0.001$.

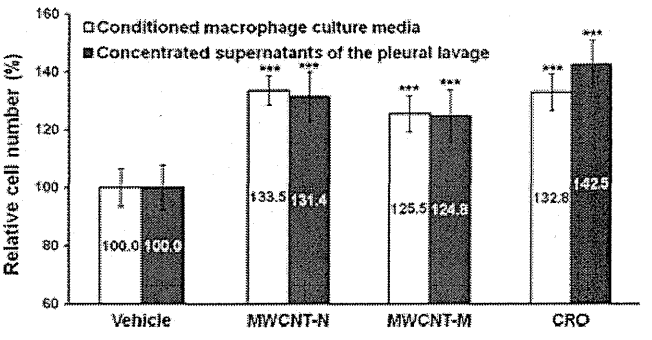

Fig. 4. Effect of conditioned macrophage culture media and the supernatants of the pleural cavity lavage (PCL) on mesothelial cell proliferation *in vitro*. The conditioned culture media of macrophages treated with multi-walled carbon nanotubes (MWCNT)-N, MWCNT-M or crocidolite (CRO) significantly increased the cell proliferation of TCC-MESO1. The concentrated supernatants of the PCL from the rats treated with MWCNT-N, MWCNT-M or CRO had similar effects. $n = 6$. $^{***}P < 0.001$.

doi: 10.1111/cas.12005

exposed to MWCNT promotes mesothelial cell proliferation *in vitro*.[30] Activated macrophages secrete a panel of growth factors and cytokines to regulate cell proliferation, which can augment transformation of mesothelial cells.[28,30,32,33] Our observations that mesothelial cell proliferation is enhanced by conditioned macrophage culture media and by the supernatants of pleural cavity lavage are consistent with these results, although the factors that are involved need to be identified.

Translocation of asbestos[34,35] and MWCNT[18] fibers from the lung to the pleural cavity has been found in rodents. This translocation also probably occurs in humans since asbestos fibers have been detected in human pleural lesions.[36] However, the mechanism and route of translocation are unclear. It has been suggested that penetration through the visceral pleura, possibly driven by increased pulmonary interstitial pressure and assisted by enhanced permeability of the visceral pleura due to asbestos-induced inflammation might be a major route.[37] In the present study, only a few MWCNT and CRO fibers were observed penetrating through the visceral pleura, and a large number of the fibers in the pleural cavity was observed in macrophages. We also observed frequent deposition of MWCNT and CRO in the mediastinal lymph nodes, mostly phagocytosed by macrophages. These results suggest that a probable route of translocation of the fibers is lymphatic flow. Inflammation in the pleural cavity is probably a defense response against translocated fibers. Murphy *et al.*[19] reported that intrapleural injection of 5 μg/mouse of long MWCNT or asbestos initiated sustained inflammation, including increased granulocyte number and protein level, in the pleural cavity. Thus, the observed proliferation of visceral mesothelial cells in the present study is probably caused by inflammatory reactions both in the lung and in the pleural cavity. In the present study, no MWCNT or crosidolite fibers or lesions were observed in the parietal pleura. This is possibly due to the short experimental period and limited amount of fibers in the pleural cavity, which would result in little inflammation in the parietal pleura.

Currently, the exposure level to MWCNT in the workplace is unknown and there are no administrational regulations for the occupational exposure limit for MWCNT. In November 2010, the National Institute of Occupational Safety and Health (NIOSH) released a non-official carbon nanotube exposure limit for peer review. The recommended exposure limit in the air was set at 7 $\mu g/m^3$.[38] Previously, we used a total dose of 1.25 mg/rat of titanium dioxide over a 9-day period and identified factors involved in titanium dioxide-induced lung lesions.[24] In the present study, we used the same protocol for the purpose of induction of observable pleural lesions and inflammation in the pleural cavity as well to ensure the presence of a detectable number of fibers in the pleural cavity after short-term administration; this dose was higher than the NIOSH exposure limit. Time- and dose-dependent experiments are needed in future studies, and further investigation is also required to elucidate cytokines and other factors that cause parietal mesothelial proliferation in animal models that are more relevant to humans.

The IPS/intratracheal instillation is a widely used method to evaluate the respiratory toxicity of particles. It should be noted that IPS/intratracheal instillation is a non-physiological method and possibly affects the migration and distribution of particles in the lung due to the pressure from spraying. However, IPS/intratracheal instillation is relevant for identifying factors to be examined using long-term, more physiologically relevant methods of CNT administration.

In summary, MWCNT and CRO fibers were found to translocate from the lung to the pleural cavity after intrapulmonary administration. Importantly, MWCNT and CRO treatment caused visceral mesothelial cell proliferation and inflammation in the pleural cavity. This mesothelial proliferation was plausibly induced by inflammatory events in the lung and pleural cavity and mediated primarily by macrophages. The similarity between MWCNT-N, MWCNT-M and CRO in translocation to the pleural cavity, induction of pleural cavity inflammation and induction of visceral pleural mesothelial proliferation suggests that MWCNT might cause asbestos-like pleural lesions.

Acknowledgments

This work was supported by Health and Labour Sciences Research Grants (Research on Risk of Chemical Substance 21340601) (grant numbers H19-kagaku-ippan-006, H22-kagaku-ippan-005).

Disclosure Statement

The authors have no conflict of interest.

References

1 Bonner JC. Nanoparticles as a potential cause of pleural and interstitial lung disease. *Proc Am Thorac Soc* 2010; **7**: 138–41.
2 Donaldson K, Murphy FA, Duffin R *et al.* Asbestos, carbon nanotubes and the pleural mesothelium: a review of the hypothesis regarding the role of long fibre retention in the parietal pleura, inflammation and mesothelioma. *Part Fibre Toxicol* 2010; **7**: 5.
3 Johnston HJ, Hutchison GR, Christensen FM *et al.* A critical review of the biological mechanisms underlying the *in vivo* and *in vitro* toxicity of carbon nanotubes: the contribution of physico-chemical characteristics. *Nanotoxicology* 2010; **4**: 207–46.
4 Nagai H, Toyokuni S. Biopersistent fiber-induced inflammation and carcinogenesis: lessons learned from asbestos toward safety of fibrous nanomaterials. *Arch Biochem Biophys* 2010; **502**: 1–7.
5 Pacurari M, Castranova V, Vallyathan V. Single- and multi-wall carbon nanotubes versus asbestos: are the carbon nanotubes a new health risk to humans? *J Toxicol Environ Health A* 2010; **73**: 378–95.
6 Tsuda H, Xu J, Sakai Y *et al.* Toxicology of engineered nanomaterials – a review of carcinogenic potential. *Asian Pac J Cancer Prev* 2009; **10**: 975–80.
7 Barrett JC. Cellular and molecular mechanisms of asbestos carcinogenicity: implications for biopersistence. *Environ Health Perspect* 1994; **102** (Suppl 5): 19–23.
8 Miller BG, Searl A, Davis JM *et al.* Influence of fibre length, dissolution and biopersistence on the production of mesothelioma in the rat peritoneal cavity. *Ann Occup Hyg* 1999; **43**: 155–66.
9 Okada F. Beyond foreign-body-induced carcinogenesis: impact of reactive oxygen species derived from inflammatory cells in tumorigenic conversion and tumor progression. *Int J Cancer* 2007; **121**: 2364–72.
10 Stanton MF, Wrench C. Mechanisms of mesothelioma induction with asbestos and fibrous glass. *J Natl Cancer Inst* 1972; **48**: 797–821.
11 Walker C, Everitt J, Barrett JC. Possible cellular and molecular mechanisms for asbestos carcinogenicity. *Am J Ind Med* 1992; **21**: 253–73.
12 Yang H, Testa JR, Carbone M. Mesothelioma epidemiology, carcinogenesis, and pathogenesis. *Curr Treat Options Oncol* 2008; **9**: 147–57.
13 Poland CA, Duffin R, Kinloch I *et al.* Carbon nanotubes introduced into the abdominal cavity of mice show asbestos-like pathogenicity in a pilot study. *Nat Nanotechnol* 2008; **3**: 423–8.
14 Sakamoto Y, Nakae D, Fukumori N *et al.* Induction of mesothelioma by a single intrascrotal administration of multi-wall carbon nanotube in intact male Fischer 344 rats. *J Toxicol Sci* 2009; **34**: 65–76.
15 Takagi A, Hirose A, Nishimura T *et al.* Induction of mesothelioma in p53+/− mouse by intraperitoneal application of multi-wall carbon nanotube. *J Toxicol Sci* 2008; **33**: 105–16.
16 Takagi A, Hirose A, Futakuchi M *et al.* Dose-dependent mesothelioma induction by intraperitoneal administration of multi-wall carbon nanotubes in p53 heterozygous mice. *Cancer Sci* 2012; **103**: 1440–4.
17 Ryman-Rasmussen JP, Cesta MF, Brody AR *et al.* Inhaled carbon nanotubes reach the subpleural tissue in mice. *Nat Nanotechnol* 2009; **4**: 747–51.
18 Mercer RR, Hubbs AF, Scabilloni JF *et al.* Distribution and persistence of pleural penetrations by multi-walled carbon nanotubes. *Part Fibre Toxicol* 2010; **7**: 28.

19 Murphy FA, Poland CA, Duffin R *et al.* Length-dependent retention of carbon nanotubes in the pleural space of mice initiates sustained inflammation and progressive fibrosis on the parietal pleura. *Am J Pathol* 2011; **178**: 2587–600.
20 Oka Y, Mitsui M, Kitahashi T *et al.* A reliable method for intratracheal instillation of materials to the entire lung in rats. *J Toxicol Pathol* 2006; **19**: 107–9.
21 Jackson P, Hougaard KS, Boisen AM *et al.* Pulmonary exposure to carbon black by inhalation or instillation in pregnant mice: effects on liver DNA strand breaks in dams and offspring. *Nanotoxicology* 2012; **6**: 486–500.
22 Morimoto Y, Hirohashi M, Ogami A *et al.* Pulmonary toxicity of well-dispersed multi-wall carbon nanotubes following inhalation and intratracheal instillation. *Nanotoxicology* 2012; **6**: 587–99.
23 Ogami A, Yamamoto K, Morimoto Y *et al.* Pathological features of rat lung following inhalation and intratracheal instillation of C(60) fullerene. *Inhal Toxicol* 2011; **23**: 407–16.
24 Xu J, Futakuchi M, Iigo M *et al.* Involvement of macrophage inflammatory protein 1alpha (MIP1alpha) in promotion of rat lung and mammary carcinogenic activity of nanoscale titanium dioxide particles administered by intrapulmonary spraying. *Carcinogenesis* 2010; **31**: 927–35.
25 Yanagihara K, Tsumuraya M, Takigahira M *et al.* An orthotopic implantation mouse model of human malignant pleural mesothelioma for *in vivo* photon counting analysis and evaluation of the effect of S-1 therapy. *Int J Cancer* 2010; **126**: 2835–46.
26 Adamson IY, Bakowska J, Bowden DH. Mesothelial cell proliferation after instillation of long or short asbestos fibers into mouse lung. *Am J Pathol* 1993; **142**: 1209–16.
27 Sekhon H, Wright J, Churg A. Effects of cigarette smoke and asbestos on airway, vascular and mesothelial cell proliferation. *Int J Exp Pathol* 1995; **76**: 411–8.
28 Adamson IY, Prieditis H, Young L. Lung mesothelial cell and fibroblast responses to pleural and alveolar macrophage supernatants and to lavage fluids from crocidolite-exposed rats. *Am J Respir Cell Mol Biol* 1997; **16**: 650–6.
29 Li XY, Lamb D, Donaldson K. Mesothelial cell injury caused by pleural leukocytes from rats treated with intratracheal instillation of crocidolite asbestos or *Corynebacterium parvum*. *Environ Res* 1994; **64**: 181–91.
30 Murphy FA, Schinwald A, Poland CA *et al.* The mechanism of pleural inflammation by long carbon nanotubes: interaction of long fibres with macrophages stimulates them to amplify pro-inflammatory responses in mesothelial cells. *Part Fibre Toxicol* 2012; **9**: 8.
31 Mutsaers SE, Whitaker D, Papadimitriou JM. Stimulation of mesothelial cell proliferation by exudate macrophages enhances serosal wound healing in a murine model. *Am J Pathol* 2002; **160**: 681–92.
32 Lechner JF, LaVeck MA, Gerwin BI *et al.* Differential responses to growth factors by normal human mesothelial cultures from individual donors. *J Cell Physiol* 1989; **139**: 295–300.
33 Wang Y, Faux SP, Hallden G *et al.* Interleukin-1beta and tumour necrosis factor-alpha promote the transformation of human immortalised mesothelial cells by erionite. *Int J Oncol* 2004; **25**: 173–8.
34 Choe N, Tanaka S, Xia W *et al.* Pleural macrophage recruitment and activation in asbestos-induced pleural injury. *Environ Health Perspect* 1997; **105** (Suppl 5): 1257–60.
35 Viallat JR, Raybuad F, Passarel M *et al.* Pleural migration of chrysotile fibers after intratracheal injection in rats. *Arch Environ Health* 1986; **41**: 282–6.
36 Kohyama N, Suzuki Y. Analysis of asbestos fibers in lung parenchyma, pleural plaques, and mesothelioma tissues of North American insulation workers. *Ann N Y Acad Sci* 1991; **643**: 27–52.
37 Miserocchi G, Sancini G, Mantegazza F *et al.* Translocation pathways for inhaled asbestos fibers. *Environ Health* 2008; **7**: 4.
38 NIOSH. Occupational exposure to carbon nanotubes and nanofibers. *Curr Intelligence Bull* 2010; **161-A**: 1–149.

Supporting Information

Additional Supporting Information may be found in the online version of this article:

Fig. S1. Characterization of multi-walled carbon nanotubes and crocidolite fibers in the suspensions.
Fig. S2. SEM observation of multi-walled carbon nanotubes and crocidolite fibers in the visceral pleura.
Fig. S3. Inflammation and fibrosis in the lung.
Fig. S4. Cytotoxicity of multi-walled carbon nanotubes and crocidolite to TCC-MESO1 cells *in vitro*.

doi: 10.1111/cas.12005

The Journal of Toxicological Sciences (J. Toxicol. Sci.)
Vol.38, No.4, 619-628, 2013

Original Article

An improved dispersion method of multi-wall carbon nanotube for inhalation toxicity studies of experimental animals

Yuhji Taquahashi, Yukio Ogawa, Atsuya Takagi, Masaki Tsuji, Koichi Morita and Jun Kanno

Division of Cellular and Molecular Toxicology, Biological Safety Research Center, National Institute of Health Sciences, 1-18-1 Kamiyoga, Setagaya-ku, Tokyo 158-8501, Japan

(Received May 5, 2013; Accepted June 9, 2013)

ABSTRACT — A multi-wall carbon nanotube (MWCNT) product Mitsui MWNT-7 is a mixture of dispersed single fibers and their agglomerates/aggregates. In rodents, installation of such mixture induces inflammatory lesions triggered predominantly by the aggregates/agglomerates at the level of terminal bronchiole of the lungs. In human, however, pulmonary toxicity induced by dispersed single fibers that reached the lung alveoli is most important to assess. Therefore, a method to generate aerosol predominantly consisting of dispersed single fibers without changing their length and width is needed for inhalation studies. Here, we report a method (designated as Taquann method) to effectively remove the aggregate/agglomerates and enrich the well-dispersed singler fibers in dry state without dispersant and without changing the length and width distribution of the single fibers. This method is base on two major concept; liquid-phase fine filtration and critical point drying to avoid re-aggregation by surface tension. MWNT-7 was suspended in Tert-butyl alcohol, freeze-and-thawed, filtered by a vibrating 25 μm mesh Metallic Sieve, snap-frozen by liquid nitrogen, and vacuum-sublimated (an alternative method to carbon dioxide critical point drying). A newly designed direct injection system generated well-dispersed aerosol in an inhalation chamber. The lung of mice exposed to the aerosol contained single fibers with a length distribution similar to the original and the Taquann-treated sample. Taquann method utilizes inexpensive materials and equipments mostly found in common biological laboratories, and prepares dry powder ready to make well-dispersed aerosol. This method and the chamber with direct injection system would facilitate the inhalation toxicity studies more relevant to human exposure.

Key words: Multi-wall carbon nanotube, Dispersion, Metallic sieve, Tert-butyl alcohol, Sublimation, Critical point drying

INTRODUCTION

We previously reported that a certain make of multi-wall carbon nanotube (MWCNT) contained particles similar to asbestos fibers in size and shape, and was positive for mesotheliomagenesis in intraperitoneal injection studies using p53-heterozygous mice (Takagi *et al.*, 2008, 2012). The intraperitoneal injection study is a specialized method for the detection of mesotheliomagenic potential of inhaled fibrous materials (Pott *et al.*, 1994; Roller *et al.*, 1997; Poland *et al.*, 2008). For the assessment of general respiratory toxicity including non-cancerous endpoints, the inhalation studies are considered essential. As a surrogate for inhalation studies, pharyngeal aspiration and intratracheal spray methods are often used. However, in both methods, the suspension medium may modify the distribution and/or the toxicity of the test particles (Morimoto *et al.*, 2011; Oyabu *et al.*, 2011; Gasser *et al.*, 2012; Wang *et al.*, 2012). Dispersion methods without suspension media are reported. However, those are usually using, at least in part of the processes, rigorous sonication or mechanical milling resulting in certain degree of physiological changes in sample characteristics, such as shortening in length distribution of MWNCT (Muller *et al.*, 2005; Mitchell *et al.*, 2007; Ahn *et al.*, 2011). Changes in particle size and/or shape will also affect the nature

Correspondence: Jun Kanno (E-mail: kanno@nihs.go.jp)

and strength of toxicity of the test substances. Therefore, development of a dispersion method to generate the aerosol of concern without addition of chemicals and changes in particle dimensions is considered to be essential for the assessment of inhalation toxicity in humans.

Fibrous nanomaterial such as Mitsui MWNT-7 is a mixture of dispersed single fibers of various length and width, and their agglomerates and aggregates. When given as a mixture, the lung lesions were mainly seen as inflammatory and/or granulomatous lesions with various degree of fibrosis at the level of terminal bronchiole accompanying the aggregates and agglomerates. These lesions were considered to block and/or mask the changes induced by the single fibers that should have reached the alveolar ducts and alveoli (Warheit *et al.,* 2004; Muller *et al.,* 2005; Shvedova *et al.,* 2008; Porter *et al.,* 2009; Mercer *et al.,* 2011; Wang *et al.,* 2011). Therefore, assessment of the toxicity of single fibers needs well-dispersed sample without aggregate/agglomerate. In practical inhalation testing, the animal chamber air is rigorously agitated in order to ensure the homogeneity of aerosol in the chamber. Therefore, if the MWNT-7 as a mixture is used, the likelihood of aggregates/agglomerates reaching the nose of the animals is high. In contrast, human ambient air is less agitated; the aggregates/agglomerates may sediment away fast and dispersed single fibers may stay longer in the air to be inhaled by humans (Han *et al.,* 2008). In addition, humans have longer respiratory tract compared to rodents and may effectively filtered out aggregates/agglomerates before the air reaches the alveolar region.

Taking all into account, we concluded that it is essential to prepare a dispersed single fiber aerosol without aggregate/agglomerates, without additional chemical components, and without changes in size and shape of the single fiber component for the rodent inhalation studies in order to predict human inhalation toxicity. To date, one dispersion method is reported, i.e. the filtration system. Filtration by a sieve with its pore size smaller than the size of aggregates/agglomerate will not affect the size distribution of the single fibers (Kasai *et al.*, 2013). However, filtration in gaseous phase turns out to be ineffective in terms of yield of the filtrate. Filtration in liquid phase is much efficient (Mercer *et al.,* 2008; Tsuda, personal communication). However, in our experience, the difficulty is found in avoiding re-aggregation during the process of drying; the surface tension. To solve this problem, here we report a new improved dispersion method consisting of a combination of aqueous filtering and the concept of a drying method used for scanning electron microscopic (SEM) samples; the critical point drying.

MATERIALS AND METHODS

MWCNT, reagent and equipments

MWCNT (Mitsui MWNT-7) was kindly donated by Mitsui & Co., Ltd., Tokyo, Japan for use in toxicity studies (Takagi *et al.,* 2008). Tert-butanol (TB) of guaranteed reagent grade was used (CAS: 75-65-0, Kanto Chemical Co., Inc., Tokyo, Japan). Metallic Sieve (pore size 25 μm mesh, Seishin Enterprise Co., LTD., Tokyo, Japan) was used for filtration. Miniature coin type vibration motors used in cellular phones (Model FM34F, T.C.P. Co, Tokyo Japan; 13,000 rpm 1.8m²/sec) are attached to the extended filler rim (5cm in depth, custom-made, Seishin Enterprise Co., LTD.) of the metallic sieve (cf. Fig. 1c) to gain high yield of filtrate. Chemistry diaphragm pumps and pumping systems (Model; MD4C NT+AK+EK, Vacuubrand, Wertheim, Germany) was used for sublimation of the frozen TB suspension and recovery of TB. Glass wares such as funnel, filtering bottle, trap bottle and silicon stoppers (Sansyo Co., Ltd., Tokyo, Japan), laboratory bottles (Pyrex®, Asahi Glass Co. Ltd., Tokyo, Japan), were used.

Dispersion method ("Taquann" method)

An outline flowchart is shown in Fig. 1. TB (melting point 25.69°C) was heated up to 60°C by a mantle heater (Sibata Scientific Technology Ltd., Saitama, Japan). It is advised not to use water bath; TB is highly hygroscopic and becomes difficult to freeze and sublimate. A volume of 200 ml of TB and 0.2 g of MWCNT were transferred to a 500 ml laboratory bottle and agitated to make crude suspension. The bottle was put into an ice bath, occasionally shaken by hand, until the suspension starts to freeze and becomes sherbet-like half frozen state and kneaded by a stainless steel spatula until it becomes evenly gray without clear crystals of TB (Fig. 1a), and then kept overnight at -25°C. To the frozen suspension, 500 ml of TB pre-heated to 60°C, was added, capped and shaken hard until the liquefied suspension becomes evenly dark brown to gray in color (Fig. 1b). The bottle was further heated up to 60°C by a mantle heater and the suspension was immediately applied to vibrating metal sieve for filtration (Fig. 1c). The filtrate was collected through a funnel into a 1,000 ml laboratory bottle. Immediately after the filtration, approximately 1,500 ml of liquid nitrogen was poured onto the filtrate in the bottle to snap freeze the suspension (Fig. 1d). Then, the bottle was connected to the pumping system and vacuumed until TB was totally sublimated; leaving dispersed MWCNT (T-CNT for Taquann-treated MWCNT) in the bottle. The MWCNT was collected by a cyclone-suction bottle using conduc-

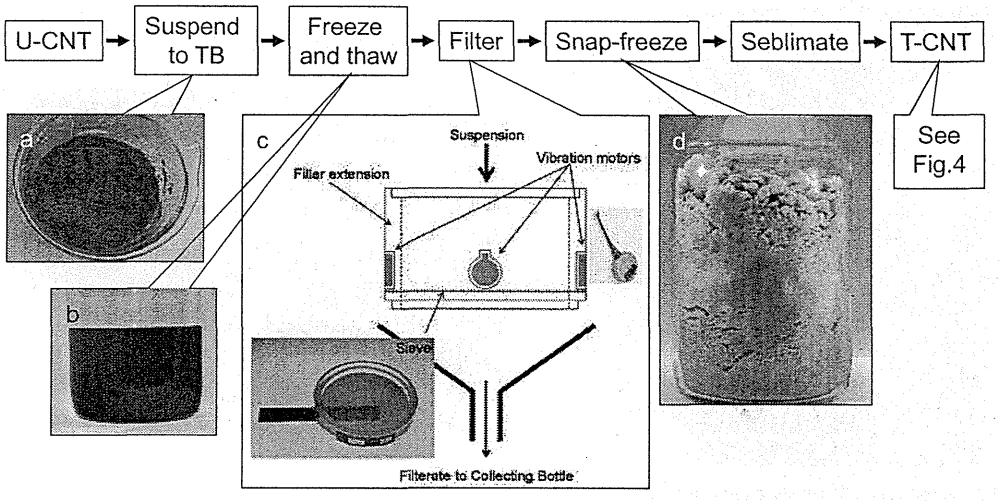

Fig. 1. Outline flowchart of the Taquann method. a) Half-frozen sherbet-like suspension of MWNT-7 kneaded (beaker was used for demonstration). b) Well-shaken liquefied suspension after adding 60°C TB (beaker was used for demonstration). c), Photograph of the sieve on a backlight box with a scale underneath (left inset), vibration motor (right inset), and a diagram of the filter unit with a filler extension and vibration motors. d) Snap-frozen filtrate.

tive silicon and aluminum tubing. In order to make a precise aliquot, a measured amount the collected T-CNT was resuspended to TB, and the suspension was aliquoted into proper containers, in this study into the newly designed cylindrical cartridge case (cf. Fig. 3), snap-frozen, and sublimated.

Aerosol generation system

An originally designed 105 L main exposure chamber (capacity of 16 mice per chamber), with a disposable electrostatic-free plastic bag inside, was prepared (Fig. 2, patent pending, manufactured by Sibata Scientific Technology Ltd.). Onto the plastic disposable top plate, a 20 L subchamber was connected with a 5 cm-diameter 10 cm long connecting pipe. To the subchamber, an injection port was connected, to which a newly designed cylindrical cartridge (manufactured by Sibata Scientific Technology Ltd.) containing dispersed T-CNT is loaded. The cartridge has a slide-valve air inlet at its base and four ejection holes at its top opening towards the subchamber lumen. The compressed air (0.8 M pascal) was injected five times with 0.2 sec duration and 10 sec interval to empty the T-CNT into the subchamber (Fig. 3). The carrier air flow from the subcamber to the main chamber was 15 L/min. Twenty-one cartridges were prepared for a two-hr exposure experiment, loading first two in 1 min for an initial boost and then one in every 6 min, resulting in generation of saw-tooth concentration wave with an average of 1.3 mg/m^3 (250 μg/cartridge) and 2.8 mg/m^3 (500 μg/cartridge).

Twelve C57BL/6NCrSlc male mice (SLC, Inc., Shizuoka, Japan), 10~11 weeks old, body weight of 23.8~30.8 g were placed in the cage suspended from the top plate of the inhalation chamber and exposed to 1 mg/m^3 of T-CNT for 2 hr a day for 5 days, lungs (excluding primary bronchi) were sampled and subjected to characterization of deposited fibers (see below).

The animal study was conducted in accordance with the Guidance for Animal Studies of the National Institute of Health Sciences under Institutional approval.

Real time particle counting and weight measurement

An optical particle counter (OPC) with a nominal detection limit of 300 nm (OPC-110GT, Sibata Scientific Technology Ltd.) and a condensation particle counter (CPC) with a nominal detection limit of 2.5 nm (ultrafine condensation particle counter 3776, Trust Science Innovation, MN, USA) were connected to the main chamber with a sample flow of 2.83 L (0.1cf) /min and 0.3 L/min respectively. The mass concentration of the chamber aerosol was calculated from the weight increase of polytetrafluoroethylene-glass fiber filter (Model T60A20, φ55mm, Tokyo Dylec Corp, Tokyo, Japan) after filtering the chamber aerosol by an Asbestos sampling pump (AIP-105, Sibata Scientific Technology Ltd.) at a rate of 1.5 L/min for 120 min (total of 180 L). Filter weight was measured by a microbalance (XP26V,

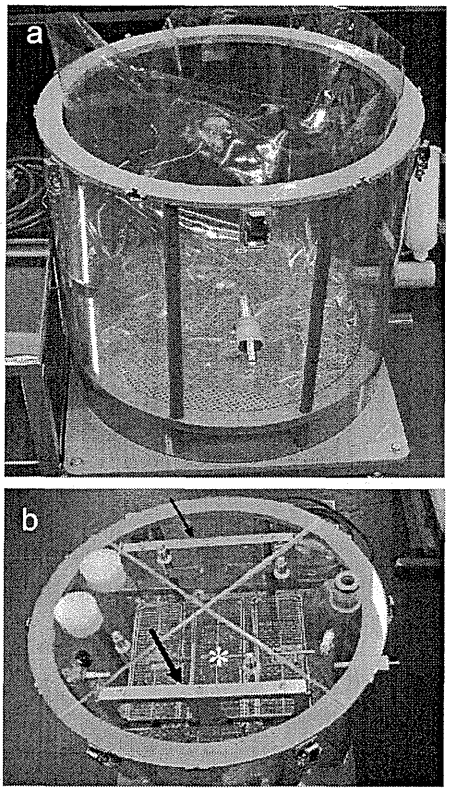

Fig. 2. Newly designed original inhalation chamber. a) Outer chamber and inner bag before top plate is in place. During operation, the space between the outer chamber and inner bag is negatively pressured to inflate the inner bag. B) Disposable top plate with tubing holes are placed on the chamber. The animal cages for 16 mice (asterisk) are suspended from the top place by a pair of hanger arms (arrows) (photo was taken without inner bag for better demonstration).

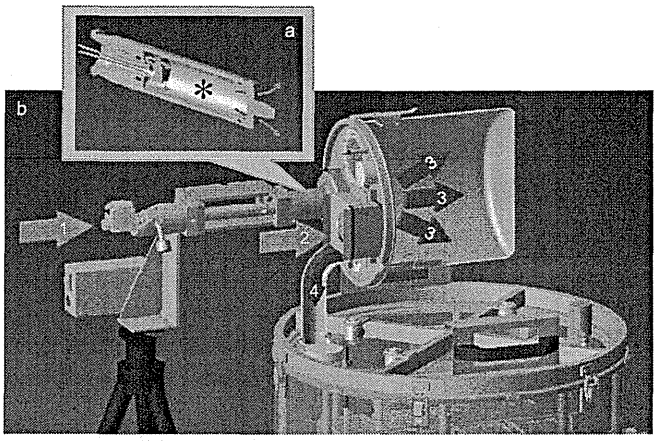

Fig. 3. A scheme of direct injection aerosol generation system. a) Upper inset shows the cut section of the injection cartridge (capacity; 23.5 ml). A slide valve opens when the cartridge is loaded to the subchamber. A measured amount of dispersed MWCNT is preloaded inside the cartridge shown in asterisk. b) Compressed air (Blue arrow 1) blows out the MWCNT through four small outlets of the cartridge into the subchamber (red arrows 3), where main flow air from the HEPA filtered inlet (blue arrow 2) mixes in. The air with the aerosol goes down the connection pipe to the main chamber (red arrow 4).

Mettler Toledo).

Characterization of the dispersed MWCNT

The T-CNT in TB suspension was mounted on a slide glass and observed under a light microscope using a pair of polarizing filters. Untreated MWCNT (U-CNT) from the bulk, 200 mg, was dispersed in to 500 ml of TB and sonicated for 30 min at 40W, 3.4 kHz (SU-3TH, Sibata Scientific Technology Ltd.) and observed.

A weight-measured aliquot of T-CNT was re-suspended, blotted on a Anopore™ Inorganic Aluminum Oxide Membrane Filters (Whatman GmbH, Dassel GE Healthcare, Hahnestrasse, Germany, pore size; 0.02 μm, φ13 mm, Anodisc 13) or a cellulose acetate/nitrocellulose membrane filter (MFTM- Millipore Membrane filters, 0.025 μm, φ13 mm, Merck Millipore, Billerica, MA, USA) and observed with a scanning electron microscope (SEM).

From the main chamber, the aerosol was collected at a rate of 5 L/min for 3 min on a Anopore™ Inorganic Aluminum Oxide Membrane Filters (Whatman GmbH, pore size; 0.1 um, Anodisc 25) joined to asbestos sampling pump (AIP-105, Sibata, Scientific Technology Ltd.). A scanning electron microscope (SEM) (VE-9800, Keyense Co., LTD., Osaka, Japan) was used for monitoring the details of the samples on the slide glasses and on the Anodiscs after osmium coating (HPC-1SW, Vacuum Device Inc., Ibaraki, Japan).

From the exposed mouse, lung lobes are collected and treated with lysis solution composed of 5 w/v% potassium hydroxide (Super Special Grade, Wako Pure Chemical Industries, Ltd., Osaka, Japan), 0.1w/v% Sodium dodecyl sulfate (SDS, for Biochemistry, Wako Pure Chemical Industries, Ltd.), 0.1 w/v% Ethylenediamine-N,N,N',N'-tetraacetic acid disodium salt dehydrate (EDTA 2Na, Dojindo laboratories, Kumamoto, Japan) and 2w/v% ascorbic acid (Super Special Grade, Wako Pure Chemical Industries, Ltd.) in ultra-pure water, dissolved at 80°C (Fig. 10b). Lung samples (approx. 200 mg) and 1.8 ml of

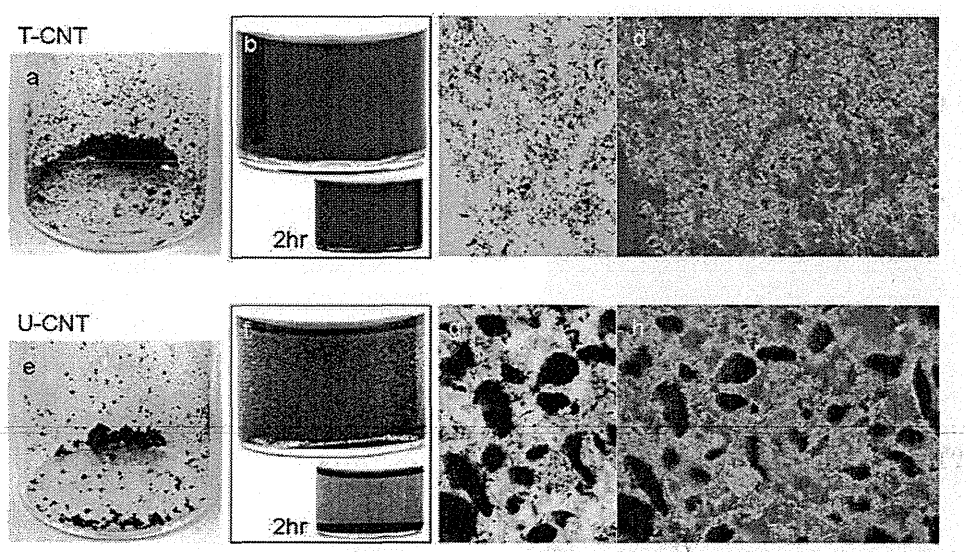

Fig. 4. Taquann-treated carbon nanotube (T-CNT) and untreated bulk carbon nanotube (U-CNT). a) final fine and dry powder of Taquann-treated MWCNT. b) Resuspended T-CNT to TB and placed for 5 min and 2 hr; T-CNT suspension is stable, compared to U-CNT, c) light microscopic view of the resuspended T-CNT on a slide glass, and d) under polarized light. e) course powder of U-CNT, f) Resuspended U-CNT to TB and placed for 5 min and 2 hr. g) light microscopic view of the resuspended U-CNT on a slide glass, and d) under polarized light. (diameter of the vials in a), b), e) and f) is 2.3 cm)

lysis solution in a centrifuge tube (DNA LoBindid tube 2.0 ml, Eppendorf, Hamburg, Germany) was incubated at 80°C for approx. 24 hr in an oven (HV-100, Funakoshi Co., Ltd., Tokyo, Japan), centrifuged at 20,000 g for 1 hr at 25°C (MX-207, Tomy Seiko Co., Ltd., Tokyo, Japan), and the pellet containing MWCNTs and SDS crystals was recovered. 1.8 ml of 70% ethanol was added to the tube and incubated at 80°C for 30 min to dissolve SDS crystals and centrifuged at 20,000 g for 1 hr at 25°C. 100 µl of 1w/w% Triton®X-100 (MP Biomedicals, Inc., Solon, OH, USA) was added to the pellet and dispersed by pipetting. One microliter of the suspension was placed on an inorganic aluminum oxide membrane filter (Anodisc 13, 0.02 µm φ13mm, Whatman GmbH) or the cellulose acetate/nitrocellulose membrane filter and filtrated on a funnel shape glass filter (SANSYO Co., LTD., Tokyo, Japan). The filter was dried at room temperature and osmium coated for SEM. For a reference of extraction efficiency, lung sample from untreated mouse was spiked with 1 µg T-CNT and measured alongside.

Lung tissue from eight mice were fixed with buffered 10% formalin (four with and four without inflation), paraffin embedded and processed routinely for H&E stained histology slides, and observed under a light microscope with or without polarizing filters (Olympus BX50 microscope with DP-70 image system, Olympus Corporation, Tokyo, Japan).

RESULTS

Characteristics of "Taquann"-dispersed MWCNT

Macroscopic and light microscopic views of the final product, the dried MWCNT after sublimation, i.e. "Taquann"-dispersed MWCNT (T-CNT) and, for comparison, untreated MWCNT from the bulk (U-CNT) are shown in Fig. 4. The powder of T-CNT is finer compared to U-CNT (Fig. 4a). The T-CNT resuspended very well to TB (Fig. 4b) and other solvents including 0.1 w/v% Sodium dodecyl sulfite and 0.1 w/v% Sodium dodecylbenzene sulfonate (not shown). Light microscopically, the resuspended T-CNT consists mostly of dispersed single fibers with smaller numbers of small aggregates corresponding to the mesh size of the metal sieve (Figs. 4c, 4d), whereas U-CNT was a mixture of large aggregates/agglomerates and single fibers among them (Figs. 4g, 4h). The T-CNT fibers slowly precipitated in the medium (cf. Figs. 4b and f), and are easily resuspended by gentle agitation. The yield of the T-CNT was approximately 5% of the U-CNT in weight. Re-filtration of the residue on the sieve resulted in negligible yield. The low power SEM views of the TB-resuspended T-CNT and U-CNT are shown in Fig. 5.

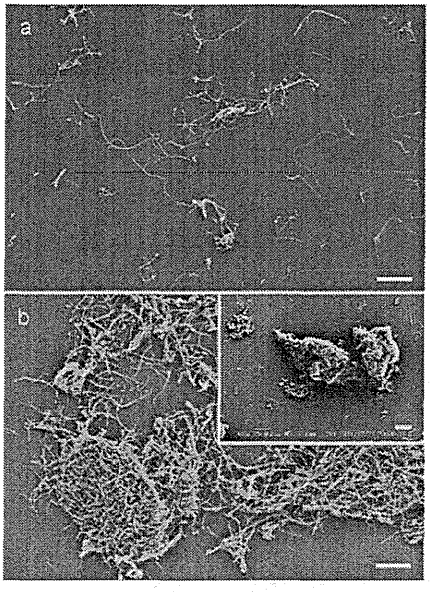

Fig. 5. Scanning electron microscopy of T-CNT and U-CNT re-suspended in TB. a) T-CNT consists mainly of dispersed single fibers with few small aggregates/agglomerates smaller than the mesh size of the sieve, SEM x 1,000. b) U-CNT showing mixture of single fibers and large aggregates/agglomerates, SEM x 1,000. The length and width distribution of the single fibers of T-CNT were virtually identical to those of U-CNT. Inset; Lower power view to demonstrate larger aggregates/agglomerates measuring up to 300 μm in major axis SEM x 400. (scale bars are 10 μm)

Again, the majority of the particles of the T-CNT were the dispersed single fibers. The length and width distribution of single fibers counted on these SEM images are shown in Fig. 6. The length and width distribution was similar between single fibers of T-CNT and U-CNT, indicating that the mechanical shortening of the fibers is negligible for Taquann method.

The number of fibers per 10, 1 and 0.1 μg weight of T-CNT with length distribution was counted on SEM images (measured number of fibers are 959, 246, and 45 per designated area for calculation, respectively). The number of fibers calculated was 2.1 x 10^7/10 μg 4.1 x 10^6/1 μg and 3.3 x 10^5/0.1 μg. The distribution of the fiber length was similar to that shown in Fig. 6a, and the average length was 7.5 ± 4.7 μm (max 34 μm), 8.7 ± 6.4 μm (max 42 μm), and 7.0 ± 5.4 μm (max 26 μm) respectively. As a whole, T-CNT has roughly 3 x 10^6 fibers per 1 μg, mean length of approximately 7 μm with a length range up to 50 μm with a median of approximately 6.5 μm.

"Taquann"-dispersed MWCNT in the inhalation chamber

The T-CNT aerosol generated at an average concentration of 1 mg/m³ was sampled on the Anodisc and observed by a SEM (Fig. 7). The aerosol was composed mainly of well-dispersed single fibers and some small tangles of fibers admixed with a relatively small amount of non-fibrous particles.

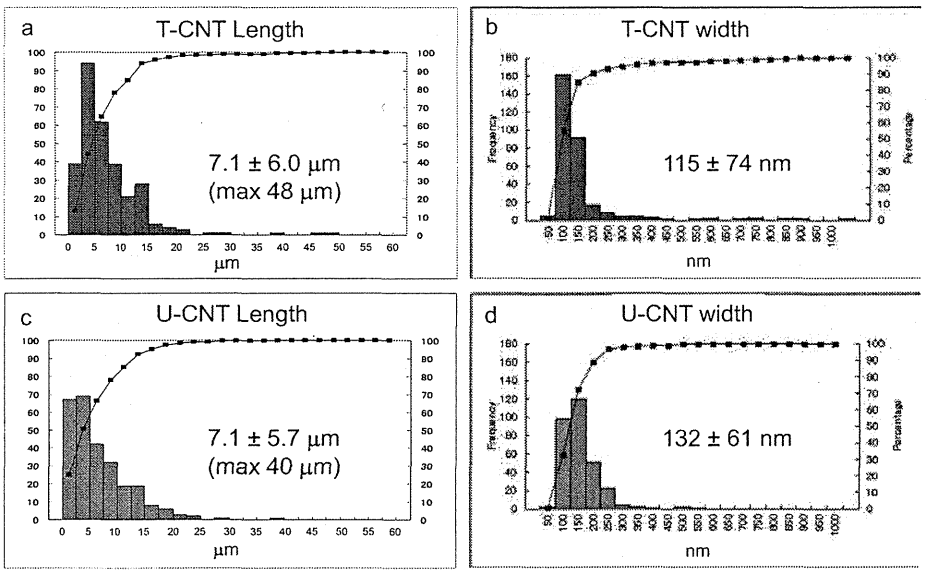

Fig. 6. Length and width of single fibers in T-CNT and U-CNT (measured by SEM on TB-resuspended samples). a) Length distribution and b) width distribution of Taquann-treated MWNT-7. c) Length distribution and d) width distribution of single fibers in the mildly sonicated suspension of the bulk MWNT-7 (mean ± s.d., n = 304 each).

Table 1. Aerosol particle count by optical particle counter (OPC) and condensation particle counter (CPC).

	Date of measurement	2013/4/29	2013/5/1	2013/5/3
Equipment	Mass concentration (mg/m³)	1.25	1.25	1.38
OPC	Average cpm* (/L) ± s.d.	627,096 ± 145,399	781,973 ± 138,610	821,272 ± 114,278
	K-value (mg/m³/cpm)	1.99 x 10^{-9}	1.60 x 10^{-9}	1.68 x 10^{-9}
CPC	Average cpm (/L) ± s.d.	859,692 ± 171,858	1,228,545 ± 223,371	1,317,873 ± 217,990
	K-value(mg/m³/cpm)	1.45 x 10^{-9}	1.02 x 10^{-9}	1.05 x 10^{-9}

*count per minute

Fig. 7. T-CNT aerosol at a concentration of 1 mg/m³ in the main chamber was collected on the Anodisc filter (5 L/min for 3 min). SEM x 1,000. (scale bar is 10 μm)

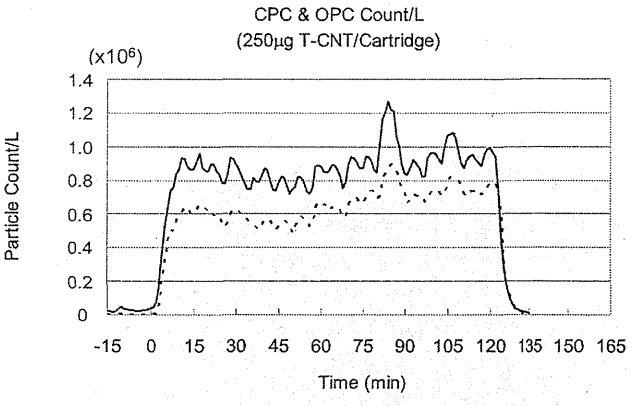

Fig. 8. A real time data from condensation particle counter (CPC, solid line) and optical particle counter (OPC, dotted line) from an inhalation chamber injected with T-CNT (250 μg/cartridge) from 0 min to 120 min with an average injection interval of 6 min (for detail see text).

From the amount of weight increase of polytetrafluoroethylene-glass fiber filter after sampling the chamber aerosol, the weight of aerosol per m³ of the chamber air (weight concentration) was calculated as approximately 1.3 mg/m³ (average of three measurements shown in Table 1). At the same time, the particle counts per m³ given by OPC and CPC were recorded (Fig. 8), and the K-value (mg/particle count in m³) was calculated (Table 1).

K-value (mg/m³/cpm), i.e. the weight concentration (mg/m³) divided by OPC or CPC count per minute (cpm) is often used as an indicator of the status of dispersion. Three measurements conducted with a few days' interval showed that not only the K-values itself but also the values used to calculate it were fairly stable over a period of days.

The length distribution of the T-CNT recovered from the lungs of two mice exposed in the whole body inhalation chamber 2 hr a day for 5 days at an average concentration of 1.8 mg/m³ of T-CNT are shown in Fig. 9 along with the data from the spiked lung tissue sample. The average length were 8.4 ± 5.0 μm and 8.3 ± 4.9 μm (Figs. 9a, 9b), comparable to that of the T-CNT in spiked lung tissue sample; 9.5 ± 5.2 μm (Fig. 9c) (width was qualitatively not different, data not shown). The total numbers of the fibers recovered were 5.1 x 10^6 and 3.2 x 10^6 from the inhaled lungs and 1.6 x 10^6 from the spiked lung; the weight of T-CNT deposited in the lung after 2 hr x 5 days of inhalation was roughly calculated as 3 μg/lung.

The fibers recovered from one of the mice were observed with SEM (Fig. 10a). Dispersed single fibers were found and some of which are longer that 20 μm (cf. Fig. 9). It was noted that EDTA and ascorbic acid in the lysis solution were effective in removing the debris from the SEM sample (Fig. 10b).

Histologically, the CNTs were found to distribute from bronchial lumen to peripheral alveolar spaces. In the bronchial lumen, the fibers were trapped in the bronchial mucus, either as single fibers or as loose aggregates

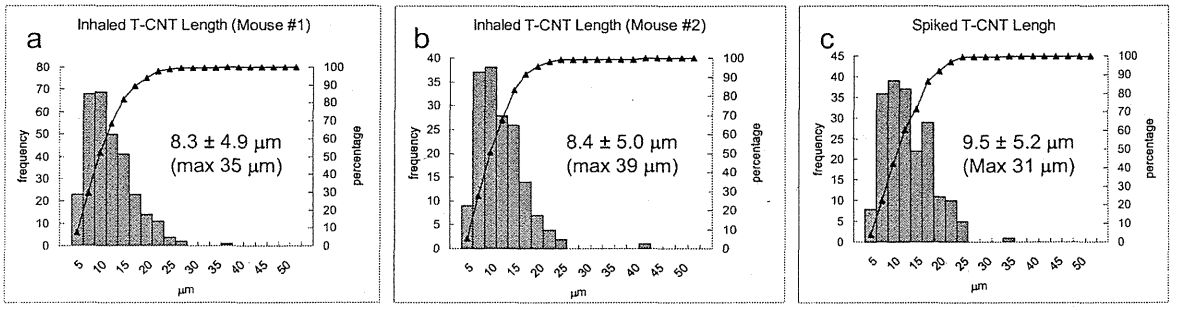

Fig. 9. T-CNT recovered from the mouse lung. a, b) Length distribution of T-CNT in the lung of two mice exposed 2 hr a day for 5 days at an average concentration of 1.8 mg/m³ (n = 306 and 166 each, mean ± s.d). c) Length distribution of T-CNT (1 μg) spiked to a non-exposed mouse lung (n = 198, mean ± s.d).

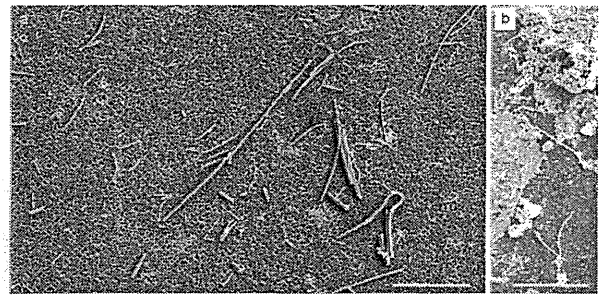

Fig. 10. T-CNT recovered from the mouse lung. a) SEM of the sediment of the dissolved lung of a mouse exposed to T-CNT in an inhalation chamber 2 hr a day for 5 days, x 2,000. Long and short single fibers are shown to be inhaled (treated with solution containing EDTA and ascorbic acid). b) SEM of a same sample treated without EDTA and ascorbic. The debris covering the fibers is considered to be iron-based amorphous substances soluble to EDTA, x 2,000. Ascorbic acid was found to be effective in keeping iron ions to be bivalent (ferrous) and soluble. (scale bars are 10 μm)

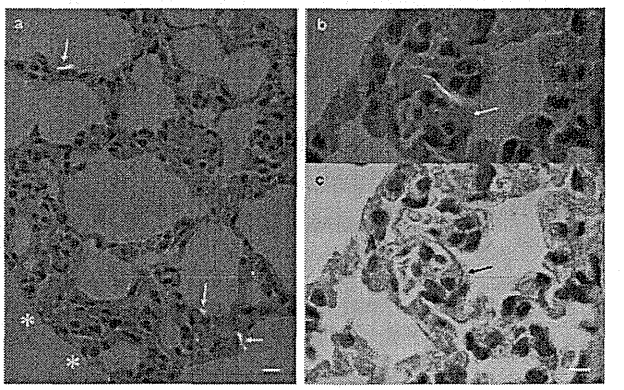

Fig. 11. a) A polarized microscopic view of the alveolar region of a lung exposed to 1 mg/m³ of T-CNT for 2 hr a day for 5 days. Arrows indicate single T-CNTs deposited in alveolar spaces phagocytized by alveolar macrophages. Asterisks indicates visceral pleural. (scale bar 10 μm) b,c) Another portion of alveolar region with a tadpole-shaped alveolar macrophage containing single long CNT in its cytoplasm shown in plain and polarized view. The lungs shown here are not inflated with formalin at fixation in order to avoid replacement of the CNTs. (scale bar 5 μm)

without inflammatory or granulomatous response, morphologically interpretable as a view of expectoration by the ciliary movement of the bronchial epithelium. There were no dense aggregates/agglomerates in the lungs so far as examined. In the peripheral alveolar space, single fibers are found phagocytized in alveolar macrophages as shown in Fig. 11. There were only mild inflammatory reactions such as neutrophilic migration against fibers in mucous blanket of the bronchial/bronchiolar segments and fibers in the alveolar space.

DISCUSSION

The MWCNT treated with the "Taquann" method (T-CNT) consisted of highly dispersed single fibers with marked reduction of aggregates/agglomerates, both in the aerosol and in the resuspended solution. The length and width distribution of the single fibers were not different between the T-CNT and the original U-CNT, indicating that this method is physically mild to the sample and does not shorten the fibers.

The Taquann method consists of two major steps, the

efficient filtration in liquid phase and the idea of critical point drying in order to prevent re-aggregation of the fibers by surface tension during drying. The latter step was inspired by the drying method for SEM samples. TB-sublimation technique used in this study is an alternative method used for SEM samples as well. Our trial-and-error added a few innovations such as gentle kneading of half-frozen TB suspension and a freeze-and-thaw process for a better dispersion (visible differences in fineness of suspension, data not shown), and vibration of the sieve for a faster and better yield of filtrate (approximately 7 fold increase in half the time). This Taquann method does not use high power sonication or other strong mechanical shearing, so that the length distribution of the single fibers did not change. The equipments and reagents used here are mostly available at regular biological or chemical laboratories. The new aerosol generating system by the direct injection of T-CNT had successfully generated highly dispersed aerosol of MWNT-7 and an exposure study confirmed the inhalation of MWNT-7 single fibers in mouse lung down to the peripheral alveolar spaces. In this condition, i.e. five consequtive days of 2 hr exposure, histologically, there were only mild neutrophilic infiltration. A long-term follow up study is underway.

It is highly plausible that the Taquann method can be applied to other types of particles as long as they are not soluble to TB (additional study in preparation). Well-dispersed samples generated by the Taquann method, together with the direct injection and the small scale inhalation chamber system, would facilitate the inhalation toxicity studies more relevant to human exposure not only at the big facilities but also at the small scaled laboratories.

Finally, this dispersion method may also be useful for industries where difficulty in dispersion of nanoparticles was a limiting process in developing new products. For a large scale manufacturing, carbon dioxide critical point drying may be suitable than TB sublimation.

ACKNOWLEDGMENT

The authors thank Dr. Hiroyuki Tsuda for introducing the metal sieve for liquid phase filtration. This study is supported by the Health Sciences Research Grants H21-kagaku-ippan-008, H23-kagaku-ippan-005 and H24-kagaku-shitei-009 from the Ministry of Health, Labour and Welfare, Japan.

REFERENCES

Ahn, K.H., Kim, S.M. and Yu, I.J. (2011): Multi-walled carbon nanotube (MWCNT) dispersion and aerosolization with hot water atomization without addition of any surfactant. Saf. Health Work., **2**, 65-69.

Gasser, M., Wick, P., Clift, M.J., Blank, F., Diener, L., Yan, B., Gehr, P., Krug, H.F. and Rothen-Rutishauser, B. (2012): Pulmonary surfactant coating of multi-walled carbon nanotubes (MWCNTs) influences their oxidative and pro-inflammatory potential in vitro. Part Fibre Toxicol., **9**, 17.

Han, J.H., Lee, E.J., Lee, J.H., So, K.P., Lee, Y.H., Bae, G.N., Lee, S.B., Ji, J.H., Cho, M.H. and Yu, I.J. (2008): Monitoring multiwalled carbon nanotube exposure in carbon nanotube research facility. Inhal. Toxicol., **20**, 741-749.

Kasai, T., Gotoh, K., Nishizawa, T., Sasaki, T., Katagiri, T., Umeda, Y., Toya, T. and Fukushima, S. (2013): Development of a new multi-walled carbon nanotube (MWCNT) aerosol generation and exposure system and confirmation of suitability for conducting a single-exposure inhalation study of MWCNT in rats. Nanotoxicology, (in press).

Mercer, R.R., Hubbs, A.F., Scabilloni, J.F., Wang, L., Battelli, L.A., Friend, S., Castranova, V. and Porter, D.W. (2011): Pulmonary fibrotic response to aspiration of multi-walled carbon nanotubes. Part Fibre. Toxicol., **8**, 21.

Mercer, R.R., Scabilloni, J., Wang, L., Kisin, E., Murray, A.R., Schwegler-Berry, D., Shvedova, A.A. and Castranova, V. (2008): Alteration of deposition pattern and pulmonary response as a result of improved dispersion of aspirated single-walled carbon nanotubes in a mouse model. Am. J. Physiol. Lung Cell. Mol. Physiol., **294**, L87-97.

Mitchell, L.A., Gao, J., Wal, R.V., Gigliotti, A., Burchiel, S.W. and McDonald, J.D. (2007): Pulmonary and systemic immune response to inhaled multiwalled carbon nanotubes. Toxicol. Sci., **100**, 203-214.

Morimoto, Y., Hirohashi, M., Ogami, A., Oyabu, T., Myojo, T., Todoroki, M., Yamamoto, M., Hashiba, M., Mizuguchi, Y., Lee, B.W., Kuroda, E., Shimada, M., Wang, W.N., Yamamoto, K., Fujita, K., Endoh, S., Uchida, K., Kobayashi, N., Mizuno, K., Inada, M., Tao, H., Nakazato, T., Nakanishi, J. and Tanaka, I. (2011): Pulmonary toxicity of well-dispersed multi-wall carbon nanotubes following inhalation and intratracheal instillation. Nanotoxicology, **6**, 587-599.

Muller, J., Huaux, F., Moreau, N., Misson, P., Heilier, J.F., Delos, M., Arras, M., Fonseca, A., Nagy, J.B. and Lison, D. (2005): Respiratory toxicity of multi-wall carbon nanotubes. Toxicol. Appl. Pharmacol., **207**, 221-231.

Oyabu, T., Myojo, T., Morimoto, Y., Ogami, A., Hirohashi, M., Yamamoto, M., Todoroki, M., Mizuguchi, Y., Hashiba, M., Lee, B.W., Shimada, M., Wang, W.N., Uchida, K., Endoh, S., Kobayashi, N., Yamamoto, K., Fujita, K., Mizuno, K., Inada, M., Nakazato, T., Nakanishi, J. and Tanaka, I. (2011): Biopersistence of inhaled MWCNT in rat lungs in a 4-week well-characterized exposure. Inhal. Toxicol., **23**, 784-791.

Poland, C.A., Duffin, R., Kinloch, I., Maynard, A., Wallace, W.A., Seaton, A., Stone, V., Brown, S., Macnee, W. and Donaldson, K. (2008): Carbon nanotubes introduced into the abdominal cavity of mice show asbestos-like pathogenicity in a pilot study. Nat Nanotechnol., **3**, 423-428.

Porter, D.W., Hubbs, A.F., Mercer, R.R., Wu, N., Wolfarth, M.G., Sriram, K., Leonard, S., Battelli, L., Schwegler-Berry, D.,

Friend, S., Andrew, M., Chen, B.T., Tsuruoka, S., Endo, M. and Castranova, V. (2009): Mouse pulmonary dose- and time course-responses induced by exposure to multi-walled carbon nanotubes. Toxicology, **269**, 136-147.

Pott, F., Roller, M., Kamino, K. and Bellmann, B. (1994): Significance of durability of mineral fibers for their toxicity and carcinogenic potency in the abdominal cavity of rats in comparison with the low sensitivity of inhalation studies. Environ. Health Perspect., **102 Suppl. 5**, 145-150.

Roller, M., Pott, F., Kamino, K., Althoff, G.H. and Bellmann, B. (1997): Dose-response relationship of fibrous dusts in intraperitoneal studies. Environ. Health Perspect., **105 Suppl. 5**, 1253-1256.

Shvedova, A.A., Kisin, E., Murray, A.R., Johnson, V.J., Gorelik, O., Arepalli, S., Hubbs, A.F., Mercer, R.R., Keohavong, P., Sussman, N., Jin, J., Yin, J., Stone, S., Chen, B.T., Deye, G., Maynard, A., Castranova, V., Baron, P.A. and Kagan, V.E. (2008): Inhalation vs. aspiration of single-walled carbon nanotubes in C57BL/6 mice: inflammation, fibrosis, oxidative stress, and mutagenesis. Am. J. Physiol. Lung Cell. Mol. Physiol., **295**, L552-565.

Takagi, A., Hirose, A., Futakuchi, M., Tsuda, H. and Kanno, J. (2012): Dose-dependent mesothelioma induction by intraperitoneal administration of multi-wall carbon nanotubes in p53 heterozygous mice. Cancer Sci., **103**, 1440-1444.

Takagi, A., Hirose, A., Nishimura, T., Fukumori, N., Ogata, A., Ohashi, N., Kitajima, S. and Kanno, J. (2008): Induction of mesothelioma in p53+/- mouse by intraperitoneal application of multi-wall carbon nanotube. J. Toxicol. Sci., **33**, 105-116.

Wang, X., Katwa, P., Podila, R., Chen, P., Ke, P.C., Rao, A.M., Walters, D.M., Wingard, C.J. and Brown, J.M. (2011): Multi-walled carbon nanotube instillation impairs pulmonary function in C57BL/6 mice. Part Fibre. Toxicol., **8**, 24.

Wang, X., Xia, T., Duch, M.C., Ji, Z., Zhang, H., Li, R., Sun, B., Lin, S., Meng, H., Liao, Y.P., Wang, M., Song, T.B., Yang, Y., Hersam, M.C. and Nel, A.E. (2012): Pluronic F108 coating decreases the lung fibrosis potential of multiwall carbon nanotubes by reducing lysosomal injury. Nano Lett., **12**, 3050-3061.

Warheit, D.B., Laurence, B.R., Reed, K.L., Roach, D.H., Reynolds, G.A. and Webb, T.R. (2004): Comparative pulmonary toxicity assessment of single-wall carbon nanotubes in rats. Toxicol. Sci., **77**, 117-125.

Xu, J., Futakuchi, M., Shimizu, H., Alexander, D.B., Yanagihara, K., Fukamachi, K., Suzui, M., Kanno, J., Hirose, A., Ogata, A., Sakamoto, Y., Nakae, D., Omori, T. and Tsuda, H. (2012): Multi-walled carbon nanotubes translocate into the pleural cavity and induce visceral mesothelial proliferation in rats. Cancer Sci., **103**, 2045-2050.

—Review—

ナノマテリアルの健康影響評価指針の国際動向

広瀬明彦

International Trend of Guidance for Nanomaterial Risk Assessment

Akihiko Hirose

Division of Risk Assessment, National Institute of Health Sciences; Kamiyoga 1-18-1, Setagaya-ku, Tokyo 158-8501, Japan.

(Received August 20, 2012)

In the past few years, several kinds of opinions or recommendations on the nanomaterial safety assessment have been published from international or national bodies. Among the reports, the first practical guidance of risk assessment from the regulatory body was published from the European Food Safety Authorities in May 2011, which included the determination of exposure scenario and toxicity testing strategy. In October 2011, European Commission (EC) adopted the definition of "nanomaterial" for regulation. And more recently, Scientific Committee on Consumer Safety of EC released guidance for assessment of nanomaterials in cosmetics in June 2012. A series of activities in EU marks an important step towards realistic safety assessment of nanomaterials. On the other hand, the US FDA announced a draft guidance for industry in June 2011, and then published draft guidance documents for both "Cosmetic Products" and "Food Ingredients and Food Contact Substances" in April 2012. These draft documents do not restrictedly define the physical properties of nanomaterials, but when manufacturing changes alter the dimensions, properties, or effects of an FDA-regulated product, the products are treated as new products. Such international movements indicate that most of nanomaterials with any new properties would be assessed or regulated as new products by most of national authorities in near future, although the approaches are still case by case basis. We will introduce such current international activities and consideration points for regulatory risk assessment.

Key words——nanomaterial; risk assessment; cosmetic product; food ingredient; food contact substance

1. はじめに

ナノマテリアルの安全性に関する国際的な関心が高まって以降，各国及び国際的な評価機関から様々なオピニオンや提言が公表されてきているが，一般的な概説やデータの収集が必要であるといったような一般論に終始しているものがほとんどであった．しかしながら最近になって，EFSA の科学委員会より 2011 年の 5 月に，より実際的なリスク評価ガイドラインが公開された．その後，化粧品や化学物質も含めて，欧米の規制当局では様々なガイダンスが公表されるようになってきている．このような国際的な動向は，現状ではケースバイケースのアプローチではあるものの，近い将来にはほとんどの新規物性を持つナノマテリアルが，ほとんどの国の規制当局によって新規物質又は新製品としてリスク評価が行われるようになることを示唆していると思われる．本稿では有害性評価の観点からの健康影響評価指針の作成に関する最近の国際動向について，特に欧州や米国の動きを中心に紹介する．

2. 欧州の動向

欧州ではナノマテリアルの安全性に関する論議は比較的活発で，欧州委員会では，2008 年に「ナノマテリアルは REACH で規制する」との基本姿勢を示しており，2009 年には，ナノマテリアルに関して Registration, Evaluation, Authorisation and Restriction of Chemicals (REACH) を実施する際の要点について具体的かつ包括的な科学的並びに技術的アドバイスを提供するための「ナノマテリアルに対する REACH 実施プロジェクト (REACH Implementation Project on Nanomaterials; RIPoN)」を開始した．2011 年 7 月には，ナノマテリアルの場合に

The author declares no conflict of interest.

国立医薬品食品衛生研究所（〒158-8501 東京都世田谷区上用賀 1-18-1)
e-mail: hirose@nihs.go.jp

本総説は，日本薬学会第 132 年会シンポジウム S25 で発表したものを中心に記述したものである．

REACHに記載すべき情報の要件（試験方法の適切さを含む）や化学的安全評価について詳細に明示したガイダンスとなる報告書の最終版を公開している.[1] 規制動向としても2009年12月に他地域より早く，欧州議会においてナノマテリアルの安全性データの届出と表示を含めた新化粧品指令（Regulation (EC) No 1223/2009）が採択されている（施行は2013年7月より）．一方，食品関係では予防原則の下に2008年12月には既存の食品添加物であっても，ナノテクノロジー等を用いて製法や粒子サイズを変更した場合は再評価が必要であることが指令（Regulation (EC) No 1333/2008）された．その後，2009年に欧州食品安全機関（European Food Safety Authority; EFSA）からナノ食品のリスクに関するオピニオンが公表された.[2]

このような状況の中2011年5月に，「食品/飼料へのナノ科学とナノテク応用から生ずる可能性のあるリスクに関するリスク評価ガイダンス」がEFSAより発表された.[3] このガイダンスではそれまでの概論的な提言とは異なり，より具体的な評価ガイダンスが示されている．その物質の物性や曝露シナリオ，化学組成としての新規性に従った以下の6つのケースを想定し，適切な毒性評価試験を組み合わせることによって具体的な評価方針を示している．

Case 1：ナノテクノロジーを利用しているが，製品中にはナノマテリアルは残存していない．

Case 2：容器等からのナノマテリアルの溶出はない．

Case 3：製品中では，完全に（適切な分析法により）非ナノサイズ（分解，溶解等）になっている．

Case 4：消化管の中で，分解することが（適切な分析法により）証明されている．

Case 5：同じ化学組成を持つ非ナノサイズの物質についての毒性情報が既に知られている場合．

Case 6：同じ化学組成を持つ非ナノサイズの物質についての毒性情報が不明な場合（全くの新規物質）．

基本的な考えとしては，Case 1–Case 4の場合においては，体内に吸収する前に非ナノサイズ物質となることで，通常の化学物質の評価手法が適用できることになると考えている．ただし，Case 4の場合は，消化管内まではナノサイズである可能性があり，刺激性などのナノマテリアルとしての局所影響を評価する必要があるとしている．そしてこれらのCaseの検討の結果，消化管内でもナノサイズである可能性が否定されない場合は，最小限の毒性試験項目として*in vitro*遺伝毒性試験と*in vivo*試験としてADME試験，90日間反復経口投与毒性試験が要求される（*in vitro*試験が陽性，又は*in vitro*試験ができない場合は*in vivo*遺伝毒性試験が必要）．これらの試験結果は，同じ化学組成を持つ非ナノサイズの物質についての毒性情報と比較され，必要に応じて更なる毒性試験を行うことが推奨されている．一方，化学組成からして全くの新規物質である場合は，ナノサイズであるなしにかかわらず，元来，慢性毒性や生殖発生毒性も含めたすべての毒性試験項目が必要となるので，上記のような曝露シナリオに依存した毒性試験の評価スキームは適用されない．

しかし現状では，食品中や消化管内等の複雑なマトリックス中のナノマテリアルのサイズを的確に測定する手法はまだ確立されておらず，安全側に立てば，ナノマテリアルが分解されないことを前提に毒性試験を行う可能性が高いこと．さらにこれまでのガイドライン化された毒性試験を適用した結果が有効であるかどうかについて，特に食品を対象とした経口投与試験について十分な知見も得られていないこと．これらの現状を考慮すると，当面はケースバイケースの対応を積み重ねていく必要があることが，今後の課題とされている．

さらに，2012年の6月には消費者安全科学委員会(Scientific Committee on Consumer Safety; SCCS)が化粧品中のナノマテリアルの評価ガイダンスを公表し，そこにも上記のような曝露シナリオに基づいた安全性評価スキームが取り入れられた.[4] こちらは主要な曝露経路が経皮曝露であるので，皮膚透過性の有無に重点が置かれているほか，局所影響としては皮膚刺激／腐蝕性，感作性，光毒性などが重要なエンドポイントとなっている．さらに，2013年7月より施行される動物実験の全面禁止を背景に，*in vitro*試験など実験動物代替試験法への取り込みが，緊急的な課題としてとりあげられている．